Published on 22 May 2012. Downloaded by UNIVERSITY OF TEESSIDE on 09/10/2014 08:42:21.

This article is published as part of the *Dalton Transactions* themed issue entitled:

Frustrated Lewis Pairs

Guest Editor: Douglas Stephan

Published in issue 30, 2012 of *Dalton Transactions*

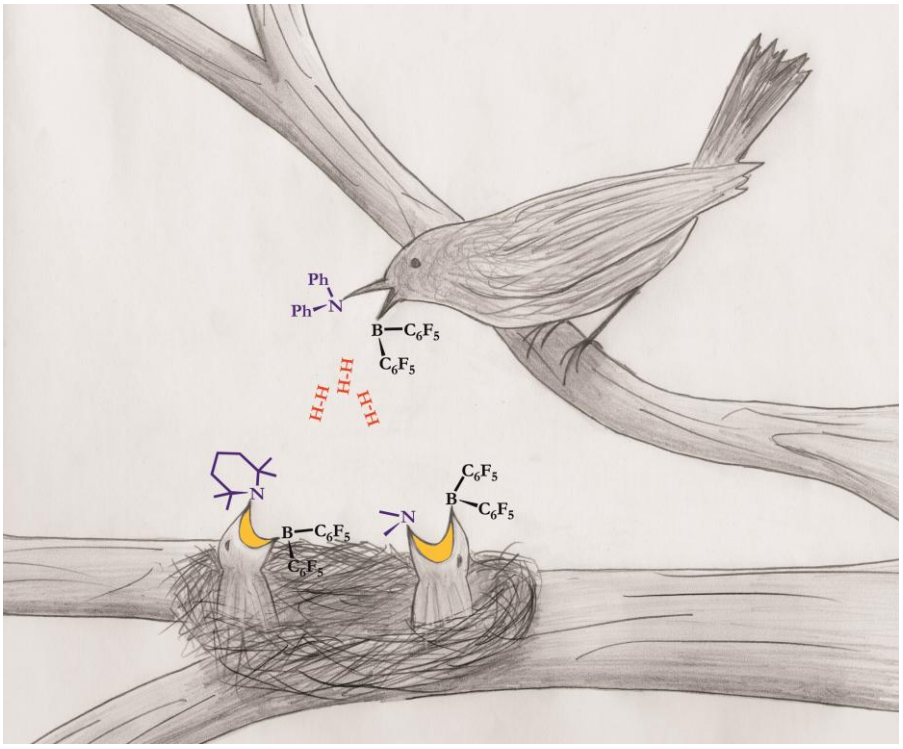

Articles in this issue include:

Communication
Hydrogen activation by 2-boryl-*N,N*-dialkylanilines: a revision of Piers' *ansa*-aminoborane
Konstantin Chernichenko, Martin Nieger, Markku Leskelä and Timo Repo

Paper
Frustrated Lewis pair addition to conjugated diynes: Formation of zwitterionic 1,2,3-butatriene derivatives
Philipp Feldhaus, Birgitta Schirmer, Birgit Wibbeling, Constantin G. Daniliuc, Roland Fröhlich, Stefan Grimme, Gerald Kehr and Gerhard Erker

Paper
Fixation of carbon dioxide and related small molecules by a bifunctional frustrated pyrazolylborane Lewis pair
Eileen Theuergarten, Janin Schlösser, Danny Schlüns, Matthias Freytag, Constantin G. Daniliuc, Peter G. Jones and Matthias Tamm

Visit the *Dalton Transactions* website for more cutting-edge inorganic chemistry research

Dalton Transactions

Dynamic Article Links

Cite this: *Dalton Trans.*, 2012, **41**, 9119

www.rsc.org/dalton

PAPER

Published on 22 May 2012. Downloaded by UNIVERSITY OF TEESSIDE on 09/10/2014 08:42:21.

Lewis pair polymerization by classical and frustrated Lewis pairs: acid, base and monomer scope and polymerization mechanism†

Yuetao Zhang,[a] Garret M. Miyake,[a] Mallory G. John,[a] Laura Falivene,[b] Lucia Caporaso,[b] Luigi Cavallo*[c] and Eugene Y.-X. Chen*[a]

Received 22nd February 2012, Accepted 23rd April 2012
DOI: 10.1039/c2dt30427a

Classical and frustrated Lewis pairs (LPs) of the strong Lewis acid (LA) $Al(C_6F_5)_3$ with several Lewis base (LB) classes have been found to exhibit exceptional activity in the Lewis pair polymerization (LPP) of conjugated polar alkenes such as methyl methacrylate (MMA) as well as renewable α-methylene-γ-butyrolactone (MBL) and γ-methyl-α-methylene-γ-butyrolactone (γ-MMBL), leading to high molecular weight polymers, often with narrow molecular weight distributions. This study has investigated a large number of LPs, consisting of 11 LAs as well as 10 achiral and 4 chiral LBs, for LPP of 12 monomers of several different types. Although some more common LAs can also be utilized for LPP, $Al(C_6F_5)_3$-based LPs are far more active and effective than other LA-based LPs. On the other hand, several classes of LBs, when paired with $Al(C_6F_5)_3$, can render highly active and effective LPP of MMA and γ-MMBL; such LBs include phosphines (*e.g.*, P^tBu_3), chiral chelating diphosphines, *N*-heterocyclic carbenes (NHCs), and phosphazene superbases (*e.g.*, P_4-^{t}Bu). The P_4-^{t}Bu/$Al(C_6F_5)_3$ pair exhibits the highest activity of the LP series, with a remarkably high turn-over frequency of 9.6×10^4 h^{-1} (0.125 mol% catalyst, 100% MMA conversion in 30 s, $M_n = 2.12 \times 10^5$ g mol^{-1}, PDI = 1.34). The polymers produced by LPs at RT are typically atactic (P_γMMBL with ~47% mr) or syndio-rich (PMMA with ~70–75% rr), but highly syndiotactic PMMA with rr ~91% can be produced by chiral or achiral LPs at −78 °C. Mechanistic studies have identified and structurally characterized zwitterionic phosphonium and imidazolium enolaluminates as the active species of the current LPP system, which are formed by the reaction of the monomer·$Al(C_6F_5)_3$ adduct with P^tBu_3 and NHC bases, respectively. Kinetic studies have revealed that the MMA polymerization by the $^tBu_3P/Al(C_6F_5)_3$ pair is zero-order in monomer concentration after an initial induction period, and the polymerization is significantly catalyzed by the LA, thus pointing to a bimetallic, activated monomer propagation mechanism. Computational study on the active species formation as well as the chain initiation and propagation events involved in the LPP of MMA with some of the most representative LPs has added our understanding of fundamental steps of LPP. The main difference between NHC and PR_3 bases is in the energetics of zwitterion formation, with the NHC-based zwitterions being remarkably more stable than the PR_3-based zwitterions. Comparison of the monometallic and bimetallic mechanisms for MMA addition shows a clear preference for the bimetallic mechanism.

Introduction

The "frustrated Lewis pair" (FLP) chemistry[1] has caught chemists' imagination and thus attracted an explosive level of recent interest since the seminal works[2] of Stephan and Erker, which introduced the FLP concept to describe sterically encumbered Lewis acid (LA, most commonly $B(C_6F_5)_3$) and Lewis base (LB, *e.g.*, P^tBu_3) pairs that are sterically precluded from forming classical donor–acceptor adducts. Instead, the unquenched, opposite LA/LB reactivity of a FLP can promote unusual reactions, or reactions that were previously known to be possible only by transition-metal complexes.[1] In its relatively short history, FLP

[a]*Department of Chemistry, Colorado State University, Fort Collins, Colorado 80523-1872, USA. E-mail: luigi.cavallo@kaust.edu.sa, eugene.chen@colostate.edu*
[b]*Dipartimento di Chimica, Università di Salerno, Via Ponte don Melillo, I-84084 Fisciano, Italy*
[c]*King Abdullah University of Science and Technology (KAUST), Chemical and Life Sciences and Engineering, Kaust Catalysis Center, Thuwal 23955-6900, Saudi Arabia*

†Electronic supplementary information (ESI) available: Cartesian coordinates with BP86 and M06 solvent phase energies. CCDC 865899 (MMA-based zwitterion **1**), 865898 (MBL-based zwitterion **2**). For ESI and crystallographic data in CIF or other electronic format see DOI: 10.1039/c2dt30427a

Published on 22 May 2012. Downloaded by UNIVERSITY OF TEESSIDE on 09/10/2014 08:42:21.

chemistry has achieved remarkable successes in many areas of chemistry, chiefly activation of small molecules,[3] catalytic hydrogenation,[4] and new reactivity/reaction development.[5]

Our interest in this area has been on the reactivity of the strongly acidic, sterically encumbered alane $Al(C_6F_5)_3$ [6] towards LB substrates and subsequent application of the resulting active species to polymerization catalysis. This interest was prompted by several surprising findings during the period of 2000–2002 in the LA/LB chemistry associated with $Al(C_6F_5)_3$, which is in sharp contrast to the LA/LB chemistry with the borane congener $B(C_6F_5)_3$. Notable examples include: (a) unique "double activation" of group 4 metallocene dimethyl bases with $Al(C_6F_5)_3$ to generate the corresponding highly active dicationic metallocene catalysts for olefin polymerization;[7] (b) formation of unusual μ-alkyl dialuminate anions from the reaction of group 5 tantalocene trimethyl with $Al(C_6F_5)_3$;[8] (c) high polymerization activity of the enolaluminate/$Al(C_6F_5)_3$ LB/LA pair *versus* inactivity of the enolborate/$B(C_6F_5)_3$ pair;[9] and (d) arene C–H bond activation taking place[10] when combining the strong LA $C_7H_8{\cdot}Al(C_6F_5)_3$ [11] with a bulky LB, 2,6-di-*tert*-butyl pyridine, which does not form a classical acid–base adduct when unsolvated $Al(C_6F_5)_3$ is used. Preceeding the current term FLP,[1] this result (d) was an early example of the unusual reactivity of the FLP relative to what was generally recognized. Since then, our interest has continued to focus on utilizing the high Lewis acidity of $Al(C_6F_5)_3$ and the unique catalytic feature of the active species derived from this alane for the polymerization of functionalized alkenes.[12] To this end, we recently communicated a significant development in this continuing effort: $Al(C_6F_5)_3$-based LPs rapidly polymerize conjugated polar alkenes, including methyl methacrylate (MMA) and naturally renewable methylene butyrolactones,[13] α-methylene-γ-butyrolactone (MBL)[14] and γ-methyl-α-methylene-γ-butyrolactone (γ-MMBL),[15] at room temperature (RT) to high molecular weight (MW) polymers.[16] The bases examined therein included phosphines [P^{t}Bu$_3$, $PMes_3$ (Mes = 2,4,6-$Me_3C_6H_2$), and PPh_3] as well as *N*-heterocyclic carbenes (NHCs), 1,3-di-*tert*-butylimidazolin-2-ylidene (I^{t}Bu) and 1,3-di-mesityl-butylimidazolin-2-ylidene (IMes). This Lewis pair polymerization (LPP) was proposed to proceed *via* zwitterionic phosphonium or imidazolium enolaluminate active species. Intriguingly, although the borane congener, $B(C_6F_5)_3$, can also form analogous zwitterionic species, it is inactive for LPP. Most recently, we found that reactive α-methylene-γ-butyrolactones (*e.g.*, MBL, γ-MMBL) can be directly and rapidly polymerized by the NHC base I^{t}Bu in DMF,[17] which represents the first conjugate-addition organopolymerization of polar alkenes by organic catalysts such as NHCs.[18]

This contribution presents a full account of our combined experimental and theoretical study on LPP, including experimental investigations into LA, LB and monomer scopes (Chart 1) and computational study of active species formation and polymerization mechanism. Notably, this study has examined a large number of classical and frustrated LPs, consisting of 11 LAs and 10 achiral and 4 chiral LBs, for the polymerization of 12 monomers of several different types, including methacrylates, an acrylate, acrylamides, α-methylene-γ-butyrolactones, a vinyl phosphonate, and cyclic monomers (lactones). Computational study of the active species formation as well as the chain initiation and propagation events involved in the polymerization of MMA by the most representative LPP systems has added our understanding of fundamental steps involved in LPP.

Experimental

Materials, reagents, and methods

All syntheses and manipulations of air- and moisture-sensitive materials were carried out in flamed Schlenk-type glassware on a dual-manifold Schlenk line, on a high-vacuum line, or in an inert gas (Ar or N_2)-filled glovebox. NMR-scale reactions were conducted in Teflon-valve-sealed J. Young-type NMR tubes. HPLC-grade organic solvents were first sparged extensively with N_2 during filling 20 L solvent reservoirs and then dried by passage through activated alumina (for Et_2O, THF, and CH_2Cl_2) followed by passage through Q-5 supported copper catalyst (for toluene and hexanes) stainless steel columns. Benzene-d_6 and toluene-d_8 were dried over sodium/potassium alloy and vacuum-distilled or filtered, whereas CD_2Cl_2 and $CDCl_3$ were dried over activated Davison 4 Å molecular sieves. NMR spectra were recorded on a Varian Inova 300 (300 MHz, ^{1}H; 75 MHz, ^{13}C; 282 MHz, ^{19}F), 400 MHz, or 500 MHz spectrometer. Chemical shifts for ^{1}H and ^{13}C spectra were referenced to internal solvent resonances and are reported as parts per million relative to $SiMe_4$, whereas ^{19}F NMR spectra were referenced to external $CFCl_3$ and ^{31}P NMR spectra to H_3PO_4.

Methyl methacrylate (MMA), furfuryl methacrylate (FMA), diethyl vinylphosphonate (DEVP), n-butyl acrylate (^{n}BA), ε-caporalactone (ε-CL), γ-valerolactone (γ-VL), γ-butyrolactone (γ-BL), and α-angelica lactone (α-AL) were purchased from Sigma-Aldrich Chemical Co, while *N*,*N*-dimethylacrylamide (DMAA), α-methylene-γ-butyrolactone (MBL), and γ-methyl-α-methylene-γ-butyrolactone (γ-MMBL) were purchased from TCI America. These monomers were first degassed and dried over CaH_2 overnight, followed by vacuum distillation; MMA was further purified by titration with neat tri(n-octyl)aluminum to a yellow end point and distillation under reduced pressure. A literature procedure was used to prepare *N*,*N*-diphenylacrylamide (DPAA).[19] The purified monomers were stored in brown bottles inside a glovebox freezer at −30 °C.

Phosphines, including PPh_3, P^{t}Bu$_3$, and $PMes_3$ were purchased from Alfa Aesar Chemical Co. Chiral phosphines, including (*S*)-(−)-(1,1′-binaphthalene-2,2′-diyl)bis(diphenylphosphine) (CP-1), (−)-1,2-bis[(2*S*,5*S*)-2,5-diisopropylphospholano]benzene (CP-2), (*S*,*S*)-1,2-bis[α-naphthyl(phenylphosphino)]ethane (CP-3), and (2*S*,3*S*)-(−)-2,3-bis(diphenylphosphino)butane (CP-4) were purchased from Sigma-Aldrich. Superbases, 1-*tert*-butyl-4,4,4-tris(dimethylamino)-2,2-bis[tris(dimethylamino)-phosphoranylidenamino]-2λ^5,4λ^5-catenadi(phosphazene) (P_4-^{t}Bu, solution in hexane) and 1-*tert*-butyl-2,2,4,4,4-pentakis(dimethylamino)-2λ^5,4λ^5-catenadi(phosphazene) (P_2-^{t}Bu, solution in THF) were purchased from Sigma-Aldrich; the solvent was removed prior to use. *N*-Heterocyclic carbenes (NHCs), including 1,3-bis(2,4,6-trimethylphenyl)imidazol-2-ylidene (IMes) and 1,3-di-*tert*-butylimidazol-2-ylidene (I^{t}Bu), were purchased from Strem Chemical Co. A literature procedure was used to prepare 1,3,4-triphenyl-4,5-dihydro-1*H*-1,2,4-triazol-5-ylidene (TPT).[20] Trimethylaluminum, triethylaluminum, and tri(n-octyl)aluminum were purchased from Strem Chemical Co., while butylated

 This journal is © The Royal Society of Chemistry 2012

Published on 22 May 2012. Downloaded by UNIVERSITY OF TEESSIDE on 09/10/2014 08:42:21.

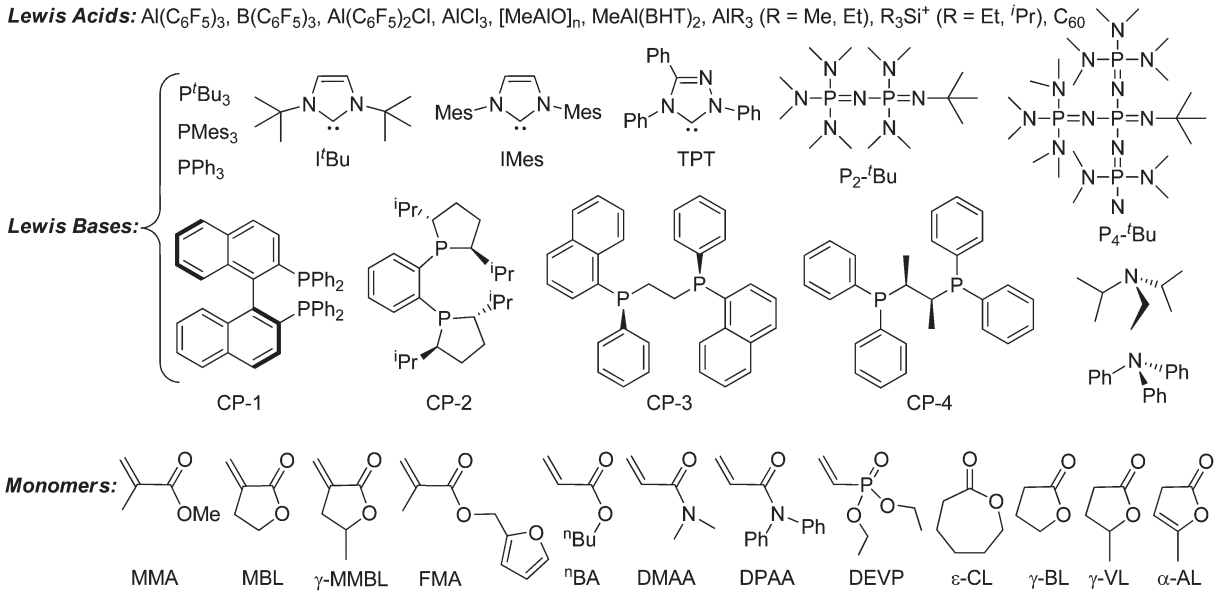

Chart 1 Scopes of LAs, LBs, and monomers investigated in this study.

hydroxytoluene (BHT-H, 2,6-di-*tert*-butyl-4-methylphenol) was purchased from Alfa Aesar Chemical Co. Methylaluminoxane solution (10 wt% in toluene, MAO), $AlCl_3$, triisopropylsilane, and triethylsilane were purchased from Aldrich Chemical Co. All chemicals were used as received unless otherwise specified as follows. C_{60} (>99.95%) was purchased from Materials Technologies Research and dried *in vacuo* prior to use. BHT-H was recrystallized from hexanes prior to use; $^tBu_3P$ was first degassed and dried over CaH_2 overnight, followed by vacuum distillation. Literature procedures were used to prepare $MeAl(BHT)_2$[21] and $Al(C_6F_5)_2Cl$.[22] Tris(pentafluorophenyl)borane, $B(C_6F_5)_3$, and activator $[Ph_3C][B(C_6F_5)_4]$[23] were obtained as research gifts from Boulder Scientific Co., and $B(C_6F_5)_3$ was further purified by recrystallization from hexanes at −30 °C. Tris(pentafluorophenyl)alane, $Al(C_6F_5)_3$, as a $(toluene)_{0.5}$ or $(toluene)_{1.0}$ adduct, or in its unsolvated form, was prepared by ligand exchange reactions between $B(C_6F_5)_3$ and $AlMe_3$ or $AlEt_3$ (for preparation of the unsolvated form).[24] (*Extra caution should be exercised when handling these materials, especially the unsolvated alane, due to its thermal and shock sensitivity!*) The $MMA{\cdot}Al(C_6F_5)_3$ adduct[9] was prepared by addition of excess MMA to a toluene solution of the alane, followed by removal of the volatiles and drying *in vacuo*; its crystal structure was determined previously.[25] Zwitterionic species derived from the reaction of $MMA{\cdot}Al(C_6F_5)_3$ with several phosphines and NHCs were previously described.[16]

Generation, NMR data, and crystal structure of MMA-based phosphonium enolaluminate $^tBu_3P$–$CH_2C(Me)$═$C(OMe)O$–$Al(C_6F_5)_3$ (1). A Teflon-valve-sealed J. Young-type NMR tube was charged with $PtBu_3$ (10.1 mg, 0.05 mmol) and 0.3 mL of C_6D_6 or CD_2Cl_2. A solution of $MMA{\cdot}Al(C_6F_5)_3$ (31.4 mg, 0.05 mmol, 0.3 mL C_6D_6 or CD_2Cl_2) was added to this tube *via* pipette at ambient temperature, and the colorless mixture was allowed to react for 10 min before analysis by NMR, which showed the clean and quantitative formation of zwitterion **1** as two isomers A (major) and B (minor) in a 7 : 3 ratio. These species undergo decomposition at RT after storing in solution for 2 h; a mixture of **1**, free $PtBu_3$, and other two unidentifiable species, but clearly no free $MMA{\cdot}Al(C_6F_5)_3$ adduct or $Al(C_6F_5)_3$ present, was formed after 20 h at RT.

^{1}H NMR (C_6D_6, 23 °C) for major isomer **1**A: δ 3.63 (s, 3H, O*Me*), 2.49 (d, J = 9.9 Hz, 2H, PCH_2), 1.70 (s, 3H,═C*Me*), 0.74 (d, J = 13.2 Hz, 27H, ^tBu); minor isomer **1**B: δ 3.27 (s, 3H, O*Me*), 2.80 (d, J = 10.8 Hz, 2H, PCH_2), 1.60 (d, J = 1.8 Hz, 3H,═C*Me*), 0.81 (d, J = 13.8 Hz, 27H, ^tBu). ^{1}H NMR (CD_2Cl_2, 23 °C) for **1**A: δ 3.50 (s, 3H, O*Me*), 3.19 (d, J = 9.6 Hz, 2H, PCH_2), 1.63 (s, br, 3H,═C*Me*), 1.52 (d, J = 13.2 Hz, 27H, ^tBu); **1**B: δ 3.23 (s, 3H, O*Me*), 3.32 (d, J = 11.1 Hz, 2H, PCH_2), 1.82 (d, J = 1.8 Hz, 3H,═C*Me*), 1.55 (d, J = 13.5 Hz, 27H, ^tBu). ^{13}C NMR (CD_2Cl_2, 23 °C) for **1**A: δ 156.5 (d, $^3J_{C-P}$ = 9.6 Hz, O*C*(OMe)═), 150.3 (dm, $^1J_{C-F}$ = 230 Hz), 141.0 (dm, $^1J_{C-F}$ = 246 Hz), 136.9 (dm, $^1J_{C-F}$ = 249 Hz), 67.78 (d, $^2J_{C-P}$ = 7.3 Hz), 52.76, 39.94 (d, $^1J_{C-P}$ = 25.9 Hz, *C*Me$_3$), 30.47 (C*Me*$_3$), 24.46 (d, $^1J_{C-P}$ = 31.8 Hz, *C*H$_2$P), 18.76 (O*Me*); **1**B: δ 160.6 (d, $^3J_{C-P}$ = 11.5 Hz, O*C*(OMe)═), 150.3 (dm, $^1J_{C-F}$ = 230 Hz), 141.0 (dm, $^1J_{C-F}$ = 246 Hz), 136.9 (dm, $^1J_{C-F}$ = 249 Hz), 75.69 (d, $^2J_{C-P}$ = 8.0 Hz), 57.49, 39.88 (d, $^1J_{C-P}$ = 26.5 Hz, *C*Me$_3$), 30.43 (C*Me*$_3$), 24.00 (d, $^1J_{C-P}$ = 33.7 Hz, *C*H$_2$P), 17.93 (O*Me*). ^{19}F NMR (C_6D_6, 23 °C) for **1**A: δ −122.6 (m, 6F, *o*-F), −156.8 (t, J_{F-F} = 21.4 Hz, 3F, *p*-F), −163.3 (m, 6F, *m*-F); **1**B: δ −122.3 (m, 6F, *o*-F), −156.9 (t, J_{F-F} = 21.4 Hz, 3F, *p*-F), −163.6 (m, 6F, *m*-F). ^{19}F NMR (CD_2Cl_2, 23 °C) for **1**A: δ −123.4 (m, 6F, *o*-F), −157.8 (t, J_{F-F} = 21.4 Hz, 3F, *p*-F), −164.3 (m, 6F, *m*-F); **1**B: δ −123.2 (m, 6F, *o*-F), −157.8 (t, J_{F-F} = 21.4 Hz, 3F, *p*-F), −164.4 (m, 6F, *m*-F). ^{31}P NMR (C_6D_6, 23 °C) for **1**A: δ 47.8 (s, P^tBu_3); **1**B: δ 51.9 (s, P^tBu_3). ^{31}P NMR (CD_2Cl_2, 23 °C) for **1**A: δ 49.0 (s, P^tBu_3); **1**B: δ 52.6 (s, P^tBu_3).

The molecular structure of **1** (*E* isomer) has been confirmed by single-crystal X-ray diffraction analysis. Single crystals suitable for X-ray diffraction analysis, obtained by layering a

Published on 22 May 2012. Downloaded by UNIVERSITY OF TEESSIDE on 09/10/2014 08:42:21.

solution of $^{t}Bu_3P$ (0.1 mmol) in 4 mL hexanes on an equimolar solution of MMA·Al(C_6F_5)$_3$ in 1 mL CH_2Cl_2 at −30 °C, were quickly covered with a layer of Paratone-N oil (Exxon, dried and degassed at 120 °C/10^{-6} Torr for 24 h) after decanting the mother liquor. A crystal was then mounted on a thin glass fiber and transferred into the cold nitrogen stream of a Bruker SMART CCD diffractometer. The structure was solved by direct methods and refined using the Bruker SHELXTL program library[26] and refined by full-matrix least-squares on F^2 for all reflections. All non-hydrogen atoms were refined with anisotropic displacement parameters, whereas hydrogen atoms were included in the structure factor calculations at idealized positions. A disordered CH_2Cl_2 solvent molecule was found in the crystal lattice, and the Platon Squeeze program was applied to take care of the solvent void (203 Å^3) in the structure refinement. The ^{t}Bu group in **1** was disordered and treated in part (C24 to C35, 59.20%; C24A to C35A, 40.80%). One perfluorophenyl ring (C13 to C18, F11 to F15, 60.36%; C13A to C18A, F11A to F15A, 39.64%) was disordered and the SAME command was implemented to restrain the bond distances and angles of the disordered perfluorophenyl ring. Selected crystallographic data for **1**: $C_{35}H_{35}AlF_{15}O_2P$, triclinic, space group $P\bar{1}$, a = 10.7749(4) Å, b = 12.9668(4) Å, c = 15.2829(5) Å, α = 92.432(2)°, β = 97.632(2)°, γ = 111.204(2)°, V = 1963.59(11) Å^3, Z = 2, D_{calcd} = 1.405 Mg m^{-3}, GOF = 1.115, R_1 = 0.0488 [$I > 2\sigma(I)$], wR_2 = 0.1545. CCDC 865899 contains the supplementary crystallographic data.

Generation, NMR data, and crystal structure of MBL-based phosphonium enolaluminate $^{t}Bu_3P$–MBL–Al(C_6F_5)$_3$ (2)

Zwitterion **2** derived from the reaction of MBL with P$^{t}Bu_3$ and toluene·Al(C_6F_5)$_3$ was carried out in the same manner as that described for **1**. ^{1}H NMR (CD_2Cl_2, 300 MHz, 23 °C): δ 4.12 (t, 2H, J = 8.5 Hz, CH_2O), 3.19 (d, 2H, J = 8.8 Hz, CH_2P), 2.67 (t, 2H, J = 8.5 Hz, CH_2CH$_2$O), 1.56 (d, 27H, J = 13.5, $^{t}Bu_3$). ^{13}C NMR (CD_2Cl_2, 23 °C): δ 163.5 (d, $^3J_{C-P}$ = 10.0 Hz, O*C*(OMe)═), 150.3 (dm, $^1J_{C-F}$ = 231 Hz), 141.0 (dm, $^1J_{C-F}$ = 246 Hz), 136.9 (dm, $^1J_{C-F}$ = 250 Hz), 66.44, 61.32 (d, $^2J_{C-P}$ = 4.6 Hz), 39.29 (d, $^1J_{C-P}$ = 26.7 Hz, *C*Me$_3$), 34.06, 30.12 (C*Me*$_3$), 19.73 (d, $^1J_{C-P}$ = 37.9 Hz, *C*H$_2$P). ^{19}F NMR (CD_2Cl_2, 282 MHz, 23 °C): δ −123.5 (m, 6F, *o*-F), −157.9 (t, J_{F-F} = 19.3 Hz, 3F, *p*-F), −164.6 (m, 6F, *m*-F). ^{31}P NMR (CD_2Cl_2, 23 °C): δ 47.4 (s, *P*$^{t}Bu_3$).

The molecular structure of **2** has been confirmed by single-crystal X-ray diffraction analysis. A 20 mL glass vial was charged with toluene·Al(C_6F_5)$_3$ (0.16 mmol), MBL (0.16 mmol), and 4 mL toluene, while another vial was charged with P$^{t}Bu_3$ (0.16 mmol) and 10 mL hexanes. The two vials were cooled to −30 °C and the solution of P$^{t}Bu_3$ was layered on the mixture of toluene·Al(C_6F_5)$_3$ and MBL *via* pipette at low temperature. The vial was stored in the freezer for one week and crystals of **2** were formed. The crystals were quickly covered with a layer of Paratone-N oil (Exxon, dried and degassed at 120 °C/10^{-6} Torr for 24 h) after decanting the mother liquor. A crystal was then mounted on a thin glass fiber and transferred into the cold nitrogen stream of a Bruker SMART CCD diffractometer. The structure was solved by direct methods and refined using the Bruker SHELXTL program library[26] and refined by full-matrix least-squares on F^2 for all reflections. All non-hydrogen atoms were refined with anisotropic displacement parameters, whereas hydrogen atoms were included in the structure factor calculations at idealized positions. Selected crystallographic data for **2**: $C_{35}H_{34}AlF_{15}O_2P$, monoclinic, space group $P2_1/n$, a = 15.9769(3) Å, b = 12.0995(2) Å, c = 18.1623(3) Å, β = 93.4810 (10)°, V = 3504.52(11) Å^3, Z = 4, D_{calcd} = 1.572 Mg m^{-3}, GOF = 1.013, R_1 = 0.0442 [$I > 2\sigma(I)$], wR_2 = 0.1483. CCDC 865898 contains the supplementary crystallographic data.

Generation and NMR data of phosphonium enolaluminate $^{t}Bu_3P$–$CH_2C(Me)$═$C(OMe)O$–$AlCl_3$ (3). A Teflon-valve-sealed J. Young-type NMR tube was charged with $AlCl_3$ (21.4 mg, 0.16 mmol) and 0.3 mL of CD_2Cl_2. MMA (16.1 mg, 0.16 mmol) was added to this tube *via* pipette at ambient temperature, and the colorless mixture was allowed to react for 10 min before analysis by NMR, which showed the clean and quantitative formation of MMA·$AlCl_3$ adduct. To this colorless solution was added P$^{t}Bu_3$ (32.5 mg, 0.16 mmol) and 0.3 mL of CD_2Cl_2. Two isomers A (major) and B (minor) in a 2 : 1 ratio were formed as predominant products. This reaction also produced other unidentified minor species, presumably a result of competing decomposition of **3** because it has limited stability at RT. A mixture containing phosphonium enolaluminate **3**, free P$^{t}Bu_3$, and some other unidentifiable species was formed after sitting the solution at RT for 36 h.

^{1}H NMR (CD_2Cl_2, 23 °C) for the MMA·$AlCl_3$ adduct: δ 6.79 (s, 1H, CH_2═), 6.28 (s, 1H, CH_2═), 4.28 (s, 3H, O*Me*), 2.09 (s, 3H,═C*Me*). ^{1}H NMR (CD_2Cl_2, 23 °C) for **3**A: δ 3.63 (s, 3H, O*Me*), 3.22 (d, J = 10.2 Hz, 2H, PCH_2), 1.83 (s, br, 3H,═C*Me*), 1.61 (d, J = 13.5 Hz, 27H, ^{t}Bu); **3**B: δ 3.60 (s, 3H, O*Me*), 3.24 (d, J = 10.8 Hz, 2H, PCH_2), 1.80 (d, J = 1.2 Hz, 3H,═C*Me*), 1.62 (d, J = 13.5 Hz, 27H, ^{t}Bu). ^{31}P NMR (CD_2Cl_2, 23 °C) for **3A**: δ 49.8 (s, *P*$^{t}Bu_3$); **3B**: δ 52.3 (s, *P*$^{t}Bu_3$).

General polymerization procedures. MMA polymerizations were performed either in 30 mL oven-dried glass reactors inside the glovebox under ambient conditions (*ca.* 25 °C) or in 25 mL oven-dried Schlenk flasks interfaced to the dual-manifold Schlenk line for runs carried out at other temperatures. A predetermined amount of a Lewis acid (LA), such as MMA·Al(C_6F_5)$_3$, (toluene)$_{0.5\ or\ 1.0}$·Al(C_6F_5)$_3$, $AlCl_3$, $AlEt_3$, $AlMe_3$, Al(C_6F_5)$_2$Cl *et al.*, was first dissolved in the monomer MMA (1.00 mL, 9.35 mmol) and 5 mL of solvent (CH_2Cl_2 or toluene) inside a glovebox, and the polymerization was started by rapid addition of a solution of a Lewis base (LB), such as phosphines PR_3, a chiral phosphines, NHCs, amines, superbases *et al.*, in 4 mL of solvent (CH_2Cl_2 or toluene) *via* a gastight syringe to the above LA + MMA solution under vigorous stirring. The amount of the monomer (M) and the [LA]/[LB] ratio (2/1) were fixed for all polymerizations, whereas the [M]/[LB] ratio was varied in some experiments. After the measured time interval, a 0.2 mL aliquot was taken from the reaction mixture *via* syringe and quickly quenched into a 4 mL vial containing 0.6 mL of undried "wet" $CDCl_3$ stabilized by 250 ppm of BHT-H; the quenched aliquots were later analyzed by ^{1}H NMR to obtain the percent monomer conversion data. The procedures for obtaining the monomer conversion data *vs.* reaction time were detailed in

 This journal is © The Royal Society of Chemistry 2012

Published on 22 May 2012. Downloaded by UNIVERSITY OF TEESSIDE on 09/10/2014 08:42:21.

literature.[25,27a] The polymerization was immediately quenched after the removal of the aliquot by addition of 5 mL 5% HCl-acidified methanol. The quenched mixture was precipitated into 100 mL of methanol, stirred for 1 h, filtered, washed with methanol, and dried in a vacuum oven at 50 °C overnight to a constant weight.

Polymerization of other monomers was performed using the same procedure already described for the MMA polymerization except for DEVP. In a typical DEVP polymerization procedure, the reactor was charged with a stir bar, a LB (P^tBu_3, PPh_3, or I^tBu), 200 equiv. of DEVP (2 mL, 0.013 mol), and 2 mL of CH_2Cl_2. The polymerization was started by rapid addition of $(toluene)_{0.5}{\cdot}Al(C_6F_5)_3$ (32.8 mg, 55.1 mmol) under vigorous stirring. The polymerization was quenched at the times specified in the polymerization table, by pouring the polymer solution into 100 mL of MeOH, and stirred for 1 h. Prior to quenching, a 0.2 mL aliquot was withdrawn from the solution and quenched into septum sealed vials containing 0.6 mL of undried "wet" $CHCl_3$ and analyzed by ^{1}H NMR for monomer conversion data. Oily polymers were collected by decanting the solvents and dried in a vacuum oven at 50 °C to a constant weight.

Polymer characterizations. Polymer number-average molecular weights (M_n) and molecular weight distributions (MWD = M_w/M_n) were measured by gel permeation chromatography (GPC) analyses carried out at 40 °C and a flow rate of 1.0 mL min^{-1}, with DMF (for PMBL and PMMBL samples) or $CHCl_3$ (for PMMA and other polymer samples) as the eluent, on a Waters University 1500 GPC instrument coupled with a Waters RI detector and equipped with four PLgel 5 μm mixed-C columns (Polymer Laboratories; linear range of molecular weight = 200–2 000 000). The instrument was calibrated with 10 PMMA standards, and chromatograms were processed with Waters Empower software (version 2002). ^{1}H NMR and ^{13}C NMR spectra for the analysis of PMMA[27,28] and PMMBL[29] microstructures were recorded and analyzed according to the literature methods.

Computational details. All the density functional theory (DFT) calculations were performed using the Gaussian09 package.[30] Geometry optimizations were performed using the BP86 GGA functional of Becke and Perdew[31] with the standard split-valence basis set with a polarization function of Ahlrichs and co-workers (SVP keyword in Gaussian).[32] Geometry optimizations were performed without symmetry constraints. Transition states (TSs) were approached through a linear transit procedure using the forming C–C bond as the reaction coordinate. Full TS searches were started from the maxima along the linear transit paths. All the geometries discussed in this work were confirmed as minima or TSs by frequency calculations. The reported energies have been obtained *via* single point energy calculations with the BP86 and M06[33] functionals with the triple-ζ basis set with one polarization function developed by Ahlrichs (TZVP keyword in Gaussian09). Solvent effects have been included in this single point energy calculation, based on the polarizable continuum solvation model PCM using toluene as the solvent.[34]

Results and discussion

Generation and characterization of $Al(C_6F_5)_3$-based zwitterionic active species

Reaction of $MMA{\cdot}Al(C_6F_5)_3$ with P^tBu_3 at RT in C_6D_6 or CD_2Cl_2 cleanly generates the corresponding zwitterionic phosphonium enolaluminate, $^tBu_3P{-}CH_2C(Me){=}C(OMe)O{-}Al(C_6F_5)_3$ (**1**), as two isomers (*E*/*Z*) in a 7 : 3 ratio (Scheme 1).[16] This addition pattern is similar to additions of FLP to non-polar substrates, such as 1,4-addition of FLPs to 1,3-dienes[35] and 1,2-addition of FLPs to terminal alkynes,[36] as well as 1,4-additions of the ethylene-bridged intramolecular frustrated P/B (phosphine/borane) Lewis pair to ynones.[37] Zwitterion **1** can be readily characterized by NMR (here using the major isomer for illustration) for the phosphonium cation [$^tBu_3P^+$][35] [δ 49.0 (s) ppm in ^{31}P NMR; 1.52 (d, ^tBu) in ^{1}H NMR], for the enolaluminate anion $[OAl(C_6F_5)_3]^-$ [25,38] [δ −123.4 (m, 6F, *o*-F), −157.8 (t, 3F, *p*-F), −164.4 (m, 6F, *m*-F) in ^{19}F NMR], and for the remaining ester enolate moiety $-CH_2C(Me){=}C(OMe)O-$ [δ 3.50 (s, 3H, O*Me*), 3.19 (d, 2H, PCH_2), 1.63 (s, 3H,=C*Me*) in ^{1}H NMR], as depicted in Fig. 1. The molecular structure (the *E* isomer) of **1** has been confirmed by X-ray diffraction analysis, as shown in Fig. 2. It is worth noting that phosphonium enolaluminate **1** starts to undergo decomposition after sitting in solution at RT for 2 h, forming a mixture containing **1**, free P^tBu_3, and other two unidentifiable species, but clearly no free $MMA{\cdot}Al(C_6F_5)_3$ or $Al(C_6F_5)_3$ present, after 20 h. Addition of excess MMA to a freshly generated solution of phosphonium enolaluminate **1** led to immediate polymerization, but the polymerization with an additional equiv. of $Al(C_6F_5)_3$ is much more rapid due to monomer activation (*vide infra*).

Intriguingly, *no reaction* took place between $PMes_3$ and $MMA{\cdot}Al(C_6F_5)_3$ at RT, although $PMes_3/Al(C_6F_5)_3$ can be described as an FLP.[16] Importantly, this observation correlates to the *non-polymerization* activity of this FLP in the presence of excess MMA (*vide infra*). On the other hand, PPh_3 and $Al(C_6F_5)_3$ cleanly form a CLP adduct, $Ph_3P{\cdot}Al(C_6F_5)_3$, but this adduct formation did not quench its reactivity toward polymerization, as this CLP is still highly active for MMA polymerization (*vide infra*); it is worth noting that the stoichiometric reaction of PPh_3 and $MMA{\cdot}Al(C_6F_5)_3$ never went to completion, and the formed zwitterionic species, $Ph_3P{-}CH_2C(Me){=}C(OMe)O{-}Al(C_6F_5)_3$ (two isomers in a 1 : 1 ratio), started to decompose at RT in less than 1 h.[16] As NHCs, such as I^tBu and IMes, are strong bases, they react with $C_7H_8{\cdot}Al(C_6F_5)_3$ at RT in benzene to form cleanly stable adducts, $I^tBu{\cdot}Al(C_6F_5)_3$ and $IMes{\cdot}Al(C_6F_5)_3$, and the reaction between I^tBu or IMes with $MMA{\cdot}Al(C_6F_5)_3$ readily generates the corresponding zwitterionic imidazolium enolaluminate active species, $I^tBu{-}CH_2C(Me){=}C(OMe)O{-}Al(C_6F_5)_3$ or $IMes{-}CH_2C(Me){=}C(OMe)O{-}Al(C_6F_5)_3$, which also correlates to the observed high polymerization activity of the $I^tBu/Al(C_6F_5)_3$ and $IMes/Al(C_6F_5)_3$ pairs in the presence of a large excess of MMA.[16] In contrast, there is no reaction between I^tBu and $B(C_6F_5)_3$ at −60 °C in toluene (*i.e.*, forming a FLP),[39] but at RT the same reaction yields a zwitterionic product with $B(C_6F_5)_3$ being attached to the 4-position of the imidazole heterocycle.[40] TPT, a weaker nucleophile than I^tBu or IMes, but still a strong base, reacts with $MMA{\cdot}Al(C_6F_5)_3$ at RT to give a mixture

Published on 22 May 2012. Downloaded by UNIVERSITY OF TEESSIDE on 09/10/2014 08:42:21.

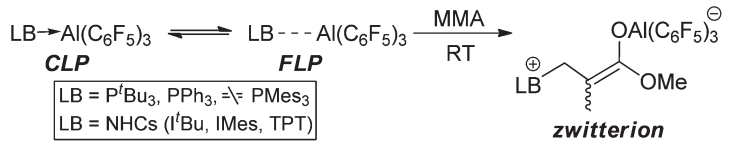

Scheme 1 $Al(C_6F_5)_3$-based classical Lewis pair (CLP) and frustrated Lewis pair (FLP) examples and their reaction with conjugated polar vinyl monomers such as MMA leading to zwitterionic species that are active for polymerization.

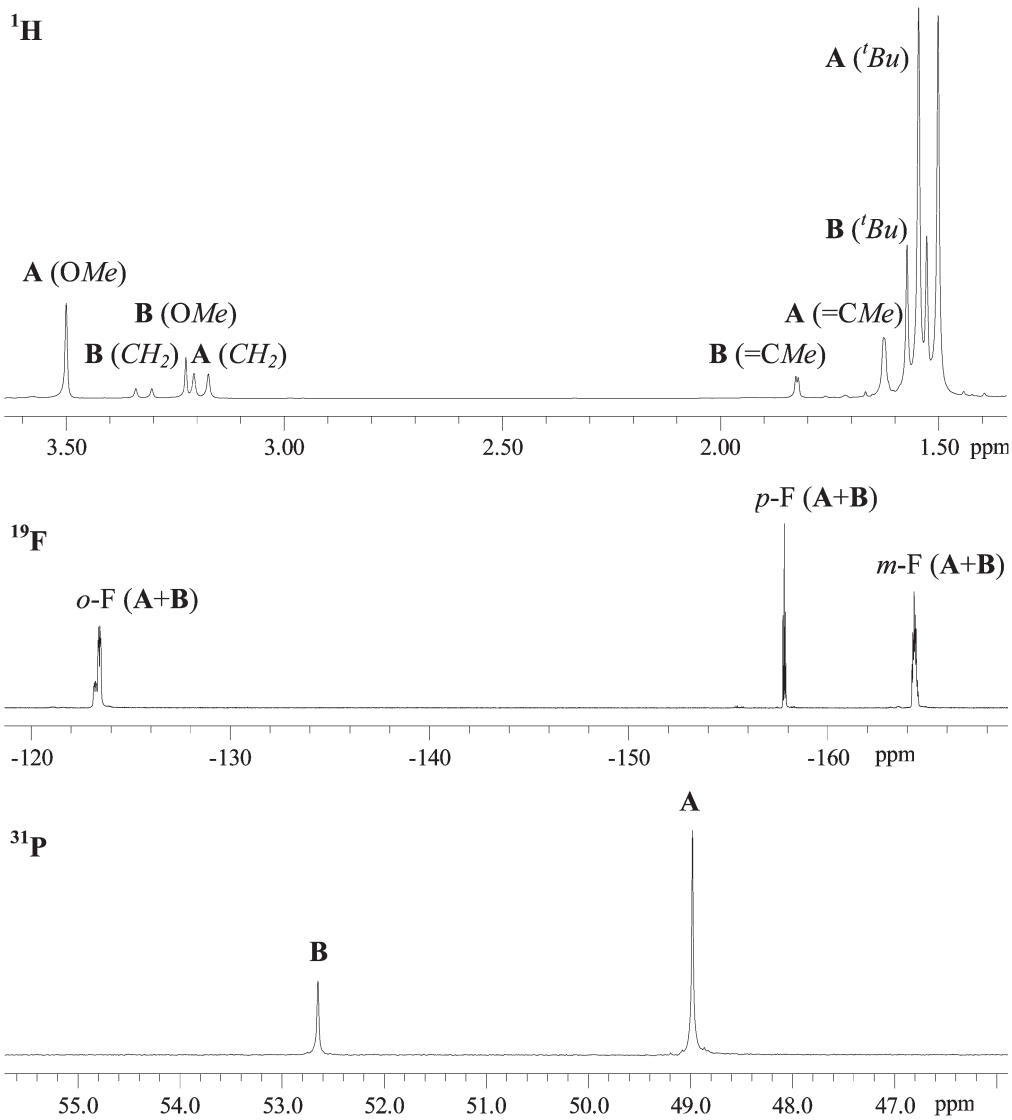

Fig. 1 ^1H, ^{19}F, and ^{31}P NMR spectra (CD_2Cl_2, 23 °C) of $^tBu_3P–CH_2C(Me)=C(OMe)O–Al(C_6F_5)_3$ (**1**) as two isomers: major isomer A and minor isomer B.

containing the zwitterionic species, PMMA, and other minor species. Nevertheless, addition of excess MMA to this mixture rapidly converted all monomer to PMMA.

Likewise, replacing MMA with the cyclic MBL having fixed *s-cis*-conformation in the reaction with the $P^tBu_3/Al(C_6F_5)_3$ pair affords the corresponding zwitterionic phosphonium enolaluminate as a single isomer (^{31}P NMR: δ 47.4), $^tBu_3P–MBL–Al(C_6F_5)_3$ (**2**). This zwitterion has been characterized spectroscopically by NMR (Fig. 3) and also structurally by X-ray diffraction analysis (Fig. 4). Also noteworthy is that phosphonium enolaluminate **2** is active for MBL polymerization, but this polymerization becomes much more rapid with an additional equiv. of $Al(C_6F_5)_3$ (*vide infra*).

Polymerization of MMA by $Al(C_6F_5)_3$/LB (LB = phosphines and NHCs) pairs. Control runs using $Al(C_6F_5)_3$ (as a toluene or MMA adduct), phosphines (P^tBu_3, $PMes_3$, and PPh_3), and NHCs (I^tBu, IMes, and TPT) individually for polymerization of MMA (200–800 equiv.) at RT in toluene yielded no polymer formation up to 24 h. (Note that TPT catalyzes tail-to-tail

 This journal is © The Royal Society of Chemistry 2012

Published on 22 May 2012. Downloaded by UNIVERSITY OF TEESSIDE on 09/10/2014 08:42:21.

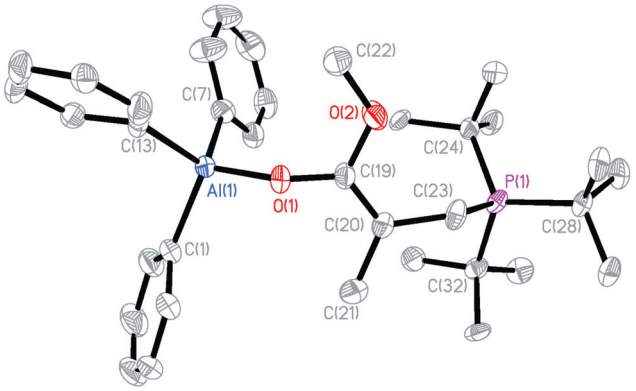

Fig. 2 X-ray crystal structure of $^{t}Bu_3P–CH_2C(Me)=C(OMe)O–Al(C_6F_5)_3$ (**1**) with thermal ellipsoids drawn at the 50% probability. Selected bond lengths (Å) and angles (°): Al(1)–O(1), 1.7513(11); O(1)–C(19), 1.3167(16); C(19)–O(2), 1.3718(18); C(19)–C(20), 1.345(2); C(20)–C(23), 1.5155(19); C(23)–P(1), 1.8487(15); Al(1)–O(1)–C(19), 142.69(11); O(1)–C(19)–C(20), 126.13(14); O(1)–C(19)–O(2), 116.33(13); O(2)–C(19)–C(20), 117.52(12); C(19)–C(20)–C(23), 118.56(13); C(20)–C(23)–P(1), 124.86(11).

dimerization of MMA in this or other solvents or in bulk at 80 °C.[41]) Premixing $C_7H_8·Al(C_6F_5)_3$ with $P^{t}Bu_3$ at RT for 10 min in either a 1 : 1 or 2 : 1 [LA]/[LB] ratio, followed by addition of MMA (800 equiv.), also led to no monomer consumption up to 24 h, due to the FLP-induced C–H activation and other decomposition of this Lewis pair.[16] On the other hand, addition of MMA (800 equiv.) to the preformed zwitterionic phosphonium enolaluminate active species **1** by pre-treating the alane–monomer adduct, $MMA·Al(C_6F_5)_3$, with this phosphine LB in toluene at RT for 10 min (*vide infra*), brought about rapid polymerization, consuming all monomer in 60 min and yielding high molecular weight (MW) polymer (M_n = 2.83 × 10^5 g mol^{-1}, polydispersity index (PDI) = M_w/M_n = 1.42; run 1, Table 1). The resulting PMMA exhibited a syndiotacticity of 75.5% rr. The same polymerization was *much more rapid* in a 2 : 1 [LA]/[LB] ratio, which converted all monomer to high MW polymer in 4 min (M_n = 3.97 × 10^5 g mol^{-1}, MWD = 1.52, rr = 73.5%, run 2), thus giving a high turn-over frequency (TOF) of 1.2 × 10^4 h^{-1}. A more convenient procedure by simply premixing $C_7H_8·Al(C_6F_5)_3$ with MMA in toluene (*i.e.*, generating $MMA·Al(C_6F_5)_3$ *in situ*), followed by addition of the base to

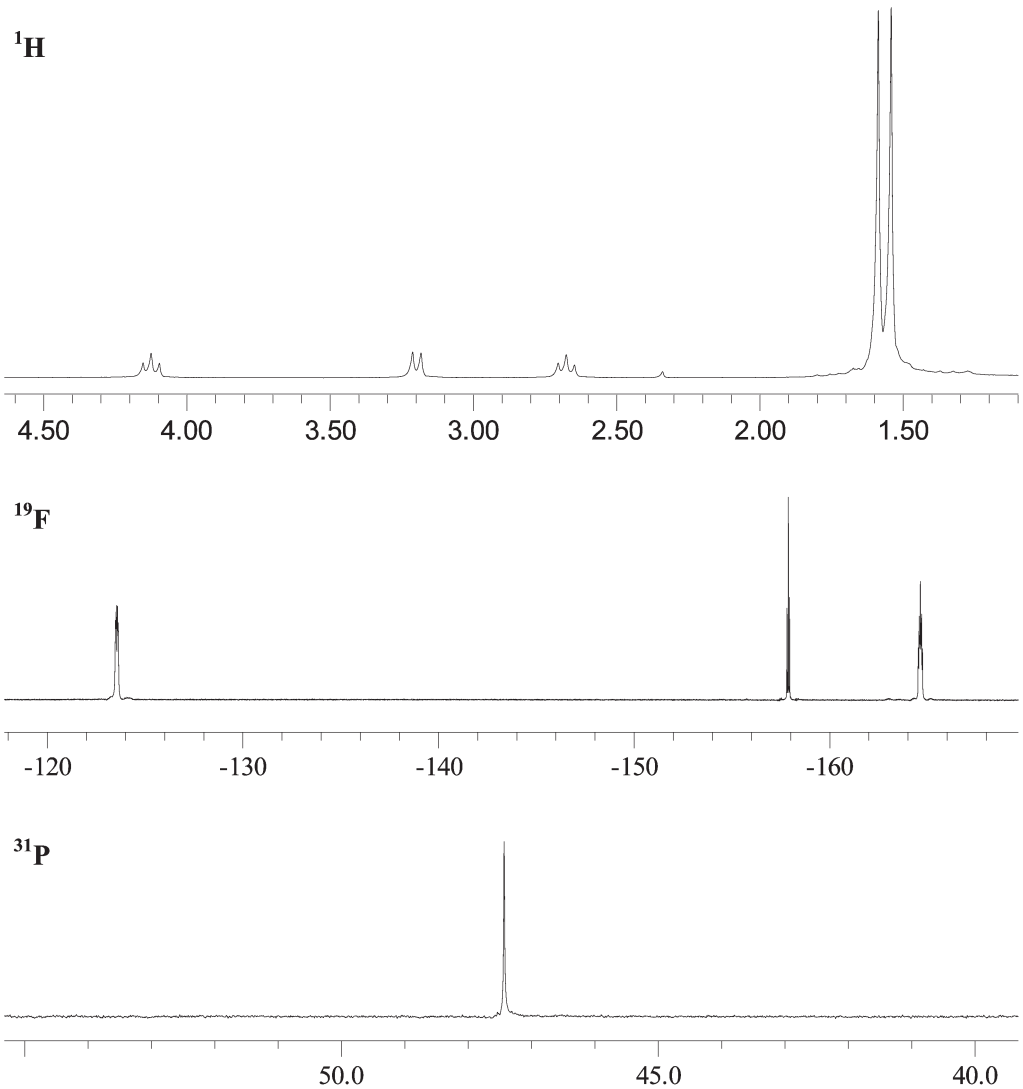

Fig. 3 ^{1}H, ^{19}F, and ^{31}P NMR spectra (CD_2Cl_2, 23 °C) of $^{t}Bu_3P–MBL–Al(C_6F_5)_3$ (**2**).

Published on 22 May 2012. Downloaded by UNIVERSITY OF TEESSIDE on 09/10/2014 08:42:21.

start the polymerization, also led to a highly active polymerization system, achieving quantitative monomer conversion in 7 min and yielding similarly high MW polymer (M_n = 3.15 × 10^5 g mol^{-1}, PDI = 1.72, rr = 73.6%, run 3). The same polymerization carried out at 0 °C was still highly effective (100% conversion in 1 h), producing PMMA with higher syndiotacticity of 77.9% rr (run 4). The PMMA with high syndiotacticity of 88.1% rr can be produced at −78 °C, at expense of polymerization activity (consuming all 80 equiv. of MMA in 100 min). Changing solvent polarity from relatively non-polar toluene (ε = 2.38) to more polar CH_2Cl_2 (ε = 8.93)[42] did not noticeably affect the polymerization activity, although there was some variation in polymer MW (run 5 *vs.* 1, 6 *vs.* 2).

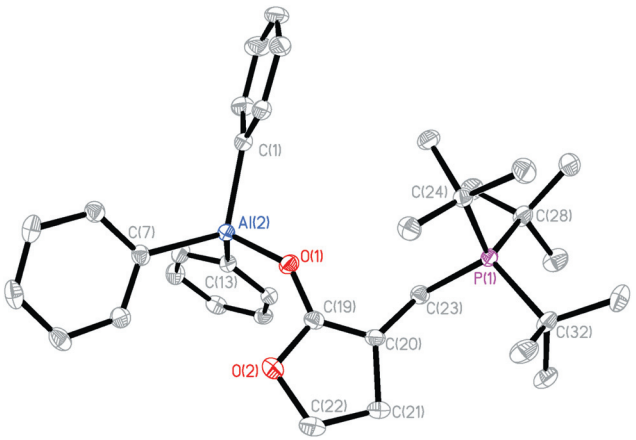

Fig. 4 X-ray crystal structure of $^tBu_3P$–MBL–$Al(C_6F_5)_3$ (**2**) with thermal ellipsoids drawn at the 50% probability. Selected bond lengths (Å) and angles (°): Al(2)–O(1), 1.7599(11); O(1)–C(19), 1.3073(17); C(19)–O(2), 1.3666(18); C(19)–C(20), 1.342(2); C(20)–C(23), 1.496(2); C(23)–P(1), 1.8332(15); Al(2)–O(1)–C(19), 138.81(10); O(1)–C(19)–C(20), 128.77(13); O(1)–C(19)–O(2), 115.97(13); O(2)–C(19)–C(20), 115.27(13); C(19)–C(20)–C(23), 120.81(13); C(20)–C(23)–P(1), 123.32(11).

Having achieved high polymerization activity with the Al$(C_6F_5)_3$/P^{t}Bu$_3$ pair using appropriate procedures (*i.e.*, by avoiding direct contact of the FLP in absence of monomer or by preforming zwitterion **1**), we examined the effectiveness of other sterically encumbered bases known to form FLPs with $B(C_6F_5)_3$. As suggested from the no reaction between $PMes_3$ and MMA·$Al(C_6F_5)_3$ at RT (*vide supra*), the $Al(C_6F_5)_3$/$PMes_3$ pair is indeed *ineffective* for MMA polymerization in toluene or CH_2Cl_2, up to 24 h (runs 7 and 8, Table 1). Interestingly, the Al$(C_6F_5)_3$/PPh_3 pair exhibits exceptional activity (TOF = 4.8 × 10^4 h^{-1}, run 9), despite the fact that PPh_3 forms a classic acid–base adduct with the alane.[16] However, the polymer produced by this pair had a bimodal MW distribution (MWD) consisting of ~41% higher MW fraction (M_n = 3.88 × 10^5 g mol^{-1}, PDI = 1.04) and ~59% lower MW fraction (M_n = 1.33 × 10^5 g mol^{-1}, PDI = 1.05), characteristic of co-existing two types of active species with rather similar catalytic activity; this polymerization behavior is consistent with the incomplete reaction of PPh_3 with MMA·$Al(C_6F_5)_3$ and instability of the resulting zwitterion (*vide supra*).

Excitingly, the $Al(C_6F_5)_3$/NHC pairs are not only extremely active for MMA polymerization (runs 10–14), they also produce PMMA with narrow and unimodal MWDs. Thus, the $Al(C_6F_5)_3$/IMes pair consumed all 800 equiv. of MMA in less than 1 min, giving a high TOF of >4.8 × 10^4 h^{-1} (run 10). In comparison, the polymerization activity of $Al(C_6F_5)_3$/I^{t}Bu is ~15 times lower, but the resulting polymer MW is ~20 times higher (M_n = 5.25 × 10^5 g mol^{-1}, PDI = 1.43, run 11) than that produced by IMes (M_n = 2.66 × 10^4 g mol^{-1}, PDI = 1.77, run 10). The polymerization by $Al(C_6F_5)_3$/I^{t}Bu in CH_2Cl_2 performed similarly to that in toluene (run 12 *vs.* 11). Likewise, the polymerization by $Al(C_6F_5)_3$/TPT in either toluene (run 13) or CH_2Cl_2 (run 14) is highly active, achieving quantitative monomer conversion in less than 1 min. An interesting and welcoming feature of the $Al(C_6F_5)_3$/TPT pair is that it produced structurally more defined polymers with considerably narrower MWDs (PDI = 1.17, run 13; PDI = 1.23, run 14) than those achieved by $Al(C_6F_5)_3$/IMes and $Al(C_6F_5)_3$/I^{t}Bu pairs.

Table 1 Selected results of MMA polymerization by $Al(C_6F_5)_3$/LB pairs [a]

Run no.	LA (adduct)	LB (1 eq.)	[LA]/[LB]	Solvent	Temp (°C)	Time (min)	Conv.[b] (%)	TOF (h^{-1})	10^{-4} M_n[c] (g mol^{-1})	PDI[c] (M_w/M_n)	[rr][d] (%)	[mr][d] (%)	[mm][d] (%)
1	Al·MMA	P^{t}Bu$_3$	1 : 1	Toluene	25	60	100	800	28.3	1.42	75.5	23.1	1.4
2	Al·MMA	P^{t}Bu$_3$	2 : 1	Toluene	25	4	100	12 000	39.7	1.52	73.5	25.0	1.5
3	Al·TOL	P^{t}Bu$_3$	2 : 1	Toluene	25	7	100	6840	31.5	1.72	73.6	24.7	1.7
4	Al·TOL	P^{t}Bu$_3$	2 : 1	Toluene	0	60	100	800	13.8	2.39	77.9	20.9	1.2
5	Al·MMA	P^{t}Bu$_3$	1 : 1	CH_2Cl_2	25	60	100	800	38.0	1.41	75.8	22.6	1.6
6	Al·MMA	P^{t}Bu$_3$	2 : 1	CH_2Cl_2	25	4	100	12 000	36.9	1.47	75.0	23.0	2.0
7	Al·MMA	$PMes_3$	2 : 1	toluene	25	1440	0	0	—	—	—	—	—
8	Al·MMA	$PMes_3$	2 : 1	CH_2Cl_2	25	1440	0	0	—	—	—	—	—
9	Al·MMA	PPh_3	2 : 1	Toluene	25	1	100	48 000	38.8; 13.3	1.04	73.0	25.4	1.6
10	Al·MMA	IMes	2 : 1	Toluene	25	1	100	48 000	2.66	1.77	72.7	25.7	1.6
11	Al·MMA	I^{t}Bu	2 : 1	Toluene	25	15	100	3200	52.5	1.43	75.1	23.3	1.6
12	Al·MMA	I^{t}Bu	2 : 1	CH_2Cl_2	25	15	100	3200	60.0	1.34	74.3	24.3	1.4
13	Al·MMA	TPT	2 : 1	Toluene	25	1	100	24 000	15.9	1.17	71.6	26.7	1.7
14	Al·MMA	TPT	2 : 1	CH_2Cl_2	25	1	100	24 000	12.5	1.23	74.2	23.7	2.1

[a] Conditions: [MMA]/[LB] = 800, except for runs 13 and 14 where LB = TPT and [MMA]/[TPT] = 400; 10 mL total solution volume. [b] Monomer conversions measured by ^{1}H NMR. [c] Number-average molecular weight (M_n) and polydispersity index (PDI) determined by GPC relative to PMMA standards. [d] Polymer methyl triads (rr, mr, mm) measured by ^{1}H NMR.

 This journal is © The Royal Society of Chemistry 2012

Published on 22 May 2012. Downloaded by UNIVERSITY OF TEESSIDE on 09/10/2014 08:42:21.

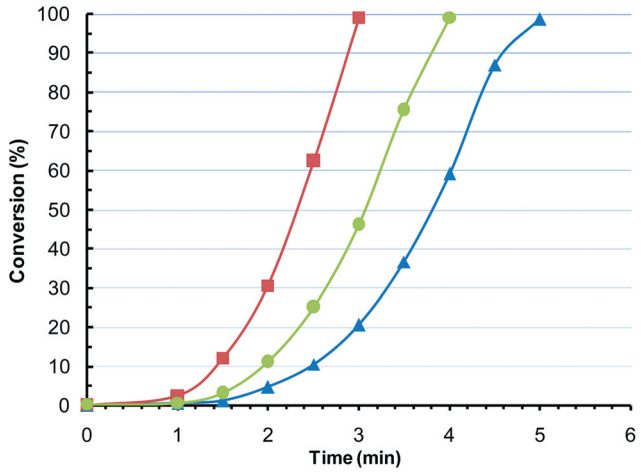

Fig. 5 Plots of monomer conversion (%) *vs.* reaction time (min) for MMA polymerization in toluene at RT by the $Al(C_6F_5)_3/P^tBu_3$ pair with two different procedures and LA catalyst concentrations. Line ▲: procedure A, [MMA]/[LA]/[LB] = 800/2/1; $[MMA]_0$ = 0.935 M, [MMA·Al $(C_6F_5)_3$] = 2.34 mM, $[P^tBu_3]$ = 1.17 mM. Line ●: procedure B, [MMA]/[LA]/[LB] = 800/1.8/1. Line ■: procedure B, [MMA]/[LA]/[LB] = 800/2/1.

Concentrating on the highly active $Al(C_6F_5)_3/P^tBu_3$ pair for polymerization of MMA, we examined kinetic profiles of the polymerization in toluene at RT using two different procedures and the LA catalyst concentrations. Specifically, in procedure A, 2 equiv. of MMA·$Al(C_6F_5)_3$ was dissolved in 800 equiv. MMA and toluene, followed by addition of 1 equiv. P^tBu_3 in toluene solution to start the polymerization. As can be seen from Fig. 5 (▲ line), after an initial slow induction period (~2 min), the monomer conversion increased almost linearly with reaction time till completion of the reaction, thus showing a zero-order dependence on [MMA]; this type of polymerization kinetics was also observed in the MMA polymerization by other nucleophile/electrophile pairs, such as zirconocene enolate/zirconocenium cation,[43] enolaluminate anion/organoaluminum,[44] and silyl ketene acetal/silylium cation[45] pairs. On the other hand, in procedure B, 1 equiv. MMA·$Al(C_6F_5)_3$ was first premixed with 1 equiv. P^tBu_3 in toluene for 10 min (to form the zwitterionic species **1**), followed by addition of another equiv. MMA·Al $(C_6F_5)_3$ + 800 equiv. of MMA, and the resulting polymerization system was considerably faster (by 55%); hence, after now a much shorter induction period (~1 min), the kinetic plot showed a linear increase of monomer conversion with time, see Fig. 5 (■ line). There also showed a significant effect of the LA concentration on the polymerization rate. For example, using the same procedure (B) but lowering the total amount of the alane from 2 equiv. to 1.8 equiv., the polymerization was slowed by 23%, see Fig. 5 (● line); consistent with this observation, increasing the amount of the alane to 2.5 equiv., the polymerization became faster by approximately 50%. These results showed that this polymerization is strongly catalyzed by LA, which is consistent with the proposed bimolecular, activated monomer propagation mechanism (*vide infra*).

Scope of monomer. To expand the utility of LPP in polymer synthesis, we examined the polymerization of 11 other monomers by $Al(C_6F_5)_3$/LB pairs, the result of which were summarized in Table 2. First, we investigated the effectiveness of $Al(C_6F_5)_3$/LB pairs for polymerization of renewable monomers MBL and γ-MMBL, cyclic analogs of MMA. Despite being a heterogeneous process (due to insolubility of the resulting polymer in the reaction medium), the polymerization of MBL by $Al(C_6F_5)_3/P^tBu_3$ in CH_2Cl_2 with [MBL]/[LB] = 800 achieved greater than 90% polymer yield in 1 h (run 1, Table 2). The PMBL produced had a medium M_n of 4.48×10^4 g mol^{-1} and a relatively high PDI of 2.18. Likewise, the $Al(C_6F_5)_3/I^tBu$ pair is also quite effective for MBL polymerization, but the M_n (which contained a small, ~4% low MW tail peak) of the resulting PMBL is ~4 times higher than that by $Al(C_6F_5)_3/P^tBu_3$ (run 2 *vs.* 1, Table 2). Owing to good solubility of PMMBL in CH_2Cl_2, the polymerization of MMBL by such LPs is homogeneous and highly effective. Specifically, the polymerization by $Al(C_6F_5)_3/P^tBu_3$ achieved quantitative monomer conversion in 10 min, giving a high MW, essentially atactic polymer ($M_n = 1.92 \times 10^5$ g mol^{-1}, PDI = 2.28, mr = 47.0%, run 3, Table 2). All LPs with three NHC bases are highly active for MMBL polymerization, with a high TOF of 4.8×10^4 h^{-1} (runs 4–6, Table 2), but M_n of 1.39×10^5 g mol^{-1} of the PMMBL produced by I^tBu is about twice of that produced by IMes, and the polymer also exhibits a much more narrow MWD (PDI = 1.15 for run 4, *vs.* PDI = 1.42 for run 5). The bimodal behavior of the LP with PPh_3 is once again manifested in the MMBL polymerization, resulting in the polymer product with ~43% high MW fraction and ~57% low MW fraction (run 7).

Neither the $Al(C_6F_5)_3/P^tBu_3$ pair nor the $Al(C_6F_5)_3$/IMes pair exhibited any reactivity toward polymerization of a bulky methacrylate, FMA, up to 24 h (runs 8–9, Table 2). Moving to an acrylate monomer, polymerization of ^{n}BA by $Al(C_6F_5)_3/P^tBu_3$ achieved 33% conversion in 1 h (run 10); however, there was no further significant increase in conversion, even after 24 h at which point the conversion was still only 35%, indicating substantial catalyst deactivation in this acrylate polymerization. On the other hand, polymerization of an acrylamide monomer, DMAA, by $Al(C_6F_5)_3/P^tBu_3$ with [DMAA]/[LB] = 800 achieved quantitative monomer conversion in 1 min, affording a high TOF of 4.8×10^4 h^{-1} and a high MW polymer with $M_n = 2.93 \times 10^5$ g mol^{-1}, PDI = 1.43 (run 11, Table 2). Likewise, the $Al(C_6F_5)_3/I^tBu$ pair is also highly active for DMAA polymerization, producing PDMAA with even higher MW of $M_n = 3.69 \times 10^5$ g mol^{-1} and lower PDI of 1.28 (run 12). In comparison, the polymerization of DPAA by $Al(C_6F_5)_3/P^tBu_3$ ([DPAA]/[LB] = 200) was much slower, requiring 24 h to achieve quantitative monomer conversion. Nonetheless, the PDPAA produced has a high MW of $M_n = 3.57 \times 10^5$ g mol^{-1} and PDI = 1.31 (run 13, Table 2). Polymerization of a vinyl phosphonate monomer, DEVP, by $Al(C_6F_5)_3/P^tBu_3$ was active but sluggish (run 14), while the polymerization by $Al(C_6F_5)_3$/IMes was significantly faster (run 15).

Moving onto cyclic esters and lactones, $Al(C_6F_5)_3/P^tBu_3$ (0.125 mol% catalyst) exhibited moderate activity toward polymerization of ε-CL, achieving 58% conversion after 20 h (run 16, Table 2). On the other hand, none of the five-membered lactones investigated, including γ-BL, γ-VL, and α-AL, were polymerized by the current LPs, such as $Al(C_6F_5)_3/P^tBu_3$ and $Al(C_6F_5)_3$/IMes, under current ambient conditions (runs 17–20, Table 2).

Published on 22 May 2012. Downloaded by UNIVERSITY OF TEESSIDE on 09/10/2014 08:42:21.

Table 2 Polymerization results by $Al(C_6F_5)_3$/LB pairs[a]

Run no.	Monomer (M)	LB (1 eq.)	[M]/[LB]	Solvent	Time (min)	Conv.[b] (%)	TOF (h^{-1})	10^{-4} M_n[c] (g mol^{-1})	PDI[c] (M_w/M_n)
1	MBL	P^tBu_3	800	CH_2Cl_2	60	(90.5)	760	4.48	2.18
2	MBL	I^tBu	800	CH_2Cl_2	60	(85.5)	704	16.3 (>96%)	1.28
3	γ-MMBL	P^tBu_3	800	CH_2Cl_2	10	100	4800	19.2	2.28
4	γ-MMBL	I^tBu	800	CH_2Cl_2	1	100	48 000	13.9	1.15
5	γ-MMBL	IMes	800	CH_2Cl_2	1	100	48 000	6.28	1.42
6	γ-MMBL	TPT	400	CH_2Cl_2	0.5	100	48 000	7.35 (>95%)	1.22
7	γ-MMBL	PPh_3	800	CH_2Cl_2	1	100	48 000	13.9; 5.01	1.03; 1.04
8	FMA	P^tBu_3	400	Toluene	1440	0	0	—	—
9	FMA	IMes	400	Toluene	1440	0	0	—	—
10	^{n}BA	P^tBu_3	800	Toluene	60	33.0	264	n.d.	n.d.
11	DMAA	P^tBu_3	800	Toluene	1	100	48 000	29.3	1.43
12	DMAA	I^tBu	800	Toluene	1.5	100	32 000	36.9	1.28
13	DPAA	P^tBu_3	200	Toluene	300	100	67	35.7	1.31
14	DEVP	P^tBu_3	200	CH_2Cl_2	1740	79.3	6	n.d.	n.d.
15	DEVP	IMes	200	CH_2Cl_2	960	75.6	10	2.79	2.11
16	ε-CL	P^tBu_3	800	Toluene	1200	58.0	23	7.37	2.76
17	γ-BL	P^tBu_3	400	Toluene	120	0	0	—	—
18	γ-BL	IMes	400	Toluene	120	0	0	—	—
19	γ-VL	P^tBu_3	400	Toluene	120	0	0	—	—
20	α-AL	P^tBu_3	400	Toluene	120	0	0	—	—

[a] Conditions: [LA]/[LB] = 2; room temperature (~25 °C); n.d. = not determined. [b] Monomer conversions measured by ^{1}H NMR; values in parentheses were isolated yields. [c] Number-average molecular weight (M_n) and polydispersity index (PDI) determined by GPC relative to PMMA standards; values (percentages) in parentheses were the percentage of the major peak when the other minor shoulder peak showed up on the GPC trace.

Table 3 Polymerization results by LA/LB pairs[a]

Run no.	LA (2 eq.)	LB (1 eq.)	Monomer (M)	[M]/[LB]	Solvent	Temp (°C)	Time (min)	Conv.[b] (%)	TOF (h^{-1})	10^{-4} M_n[c] (g mol^{-1})	PDI[c] (M_w/M_n)	[rr][d] (%)
1	$B(C_6F_5)_3$	P^tBu_3	MMA	400	Toluene	25	1440	0	0	—	—	—
2	$MeAl(BHT)_2$	P^tBu_3	MMA	800	Toluene	25	1440	0	0	—	—	—
3	$AlMe_3$	P^tBu_3	MMA	400	Toluene	25	1440	Trace	~0	—	—	—
4	$AlEt_3$	PPh_3	MMA	40	Toluene	25	1440	97.3	1.6	1.17	2.25	67.8
5	$AlEt_3$	PPh_3	MMA	40	Toluene	–78	1440	100	1.7	3.86	1.60	87.5
6	$AlCl_3$	P^tBu_3	MMA	800	Toluene	25	1440	66.7	22	2.55	1.91	68.9
7	$AlCl_3$	P^tBu_3	MMA	800	Toluene	–78	600	100	80	27.3	2.12	91.1
8	$ClAl(C_6F_5)_2$	P^tBu_3	MMA	400	Toluene	25	1440	32.8	5.5	1.84 (98%)	1.42	n.d.
9	$ClAl(C_6F_5)_2$	IMes	MMA	400	Toluene	25	1440	36.4	6.1	0.52	1.43	n.d.
10	$ClAl(C_6F_5)_2$	P^tBu_3	γ-MMBL	400	CH_2Cl_2	25	1440	22.5	3.8	1.64 (98%)	1.36	n/a
11	$ClAl(C_6F_5)_2$	IMes	γ-MMBL	400	CH_2Cl_2	25	1440	45.4	7.6	2.47	2.06	n/a
12	MAO	none	γ-MMBL	n.a.	CH_2Cl_2	25	1440	30.6	n/a	1.35 (99%)	1.29	n/a
13	MAO	P^tBu_3	γ-MMBL	400	CH_2Cl_2	25	1440	93.2	15	0.79 (99%)	1.26	n/a
14	MAO	I^tBu	γ-MMBL	400	CH_2Cl_2	25	1440	95.6	16	0.79 (99%)	1.27	n/a
15	Et_3Si^+	P^tBu_3	MMA	400	CH_2Cl_2	25	1440	0	0	—	—	—
16	$^iPr_3Si^+$	P^tBu_3	MMA	400	CH_2Cl_2	25	1440	0	0	—	—	—
17	C_{60}	IMes	MMA	800	Toluene	25	1440	0	0	—	—	—
18	C_{60}	I^tBu	γ-MMBL	200	DMF	25	1080	0	0	—	—	—

[a] Conditions: [LA]/[LB] = 2, except for runs by MAO (12–14) where 100 equiv. was used. Silylium ions $R_3Si^+[B(C_6F_5)_4]^-$ were generated *in situ* from R_3SiH + $Ph_3C[B(C_6F_5)_4]$. n/a = not applicable; n.d. = not determined. [b] Monomer conversions measured by ^{1}H NMR. [c] Number-average molecular weight (M_n) and polydispersity index (PDI) determined by GPC relative to PMMA standards; values (percentages) in parentheses were the percentage of the major peak when the other minor (trace) shoulder peak showed up on the GPC trace. [d] Polymer methyl triads (rr, mr, mm) measured by ^{1}H NMR.

Scope of Lewis acids and bases. As described above, LPs based on the strong LA $Al(C_6F_5)_3$ are highly active for polymerization of conjugated polar alkenes such as methacrylates, acrylamides, and α-methylene-γ-butyrolactones. An interesting fundamental and practical question is whether this LA could be replaced by other more common LAs without compromising polymerization activity. To address this question, we initially examined common LAs such as $B(C_6F_5)_3$, $MeAl(BHT)_2$, and $AlMe_3$, in combination with the highly effective LB partner, P^tBu_3, for MMA polymerization, but observed none to negligible polymer formation, up to 24 h (runs 1–3, Table 3). The finding of the inactivity of the $B(C_6F_5)_3/P^tBu_3$ pair, even with another equiv. of $B(C_6F_5)_3$, is intriguing because MMA·$B(C_6F_5)_3$ readily reacts with P^tBu_3 to form zwitterionic phosphonium enolborate $^tBu_3P$–$CH_2C(Me)$=$C(OMe)O$–$B(C_6F_5)_3$.[16] This observation is reminiscent of our previous findings regarding the high activity of enolaluminate *vs.* inactivity of enolborate species toward conjugate-addition polymerization, attributed to

 This journal is © The Royal Society of Chemistry 2012

Published on 22 May 2012. Downloaded by UNIVERSITY OF TEESSIDE on 09/10/2014 08:42:21.

the inability of the enolborate/borane pair to effect the bimolecular, activated-monomer anionic polymerization as does the enolaluminate/alane pair.[9,38] With a 10-fold increase in the LP loading (2.5 mol%), the $AlEt_3/PPh_3$ pair is active for MMA polymerization at both RT and −78 °C, albeit the TOF numbers were low (<2 h^{-1}, runs 4–5), which is consistent with the results reported by Hatada *et al.*[46] The syndiotacticity of the PMMA produced at −78 °C, 87.5% rr, is considerably higher than that produced at RT, 67.8% rr, so is the polymer molecular weight (run 5 *vs.* 4).

For LPP of MMA, $AlCl_3$ is much more effective than AlR_3. Thus, even in a low catalyst loading of 0.125 mol%, the $AlCl_3/P^tBu_3$ pair exhibited modest activity in MMA polymerization, achieving 66.7% conversion in 24 h (run 6). Kinetic profiling of this polymerization showed that 66.4% conversion was already achieved within 1.5 min and there was no noticeable increase in conversion thereafter (up to 24 h), the observation of which indicated rapid catalyst deactivation, as indicated by the instability of the $AlCl_3$-derived zwitterionic species (see Experimental). Keeping this in mind, we ran the same polymerization at −78 °C and achieved quantitative monomer conversion in 10 h (run 7). More significantly, the MW of the PMMA produced at −78 °C (M_n = 2.73 × 10^5 g mol^{-1}) is more than 10 times higher than that produced at RT (run 7 *vs.* 6). Impressively, this low temperature polymerization produced highly syndiotactic PMMA (91.1% rr).

Compared to $Al(C_6F_5)_3$, $ClAl(C_6F_5)_2$ based LPs are much less active for both polymerizations of MBL and γ-MMBL (runs 8–11, Table 3). Specifically, the $ClAl(C_6F_5)_2$/LB pairs achieved low monomer conversions of <50%, even after extended times (14 h). Based on kinetic profiling experiments, there was substantial catalyst deactivation after an initial stage of polymerization (1 min), after which no significant increase in monomer conversion occurred. Considering methylaluminoxane (MAO) as a potent Lewis acidic activator for olefin polymerization by metal-based catalysts,[47] we examined MAO-based LPs for γ-MMBL polymerization. In absence of a LB, MAO (100 equiv.) itself is active for γ-MMBL (400 equiv.) polymerization at RT, achieving 30.6% conversion after 24 h (run 12). With an additional of 1 equiv. of P^tBu_3, the conversion was enhanced to 93.2% in the same period, producing the polymer with a relatively low MW of M_n = 7.89 × 10^3 g mol^{-1} (run 13, Table 3). Using an NHC base, the MAO/I^{t}Bu pair performed similarly in this polymerization (run 14 *vs.* 13, Table 3).

Interestingly, strongly Lewis acidic silylium ions R_3Si^+-$[B(C_6F_5)_4]^-$, generated *in situ* from the reaction of R_3SiH + $Ph_3C[B(C_6F_5)_4]$, are inactive as LAs for LPP of MMA polymerization in either toluene or CH_2Cl_2 at RT, when combined with P^tBu_3 (runs 15–16, Table 3). We also examined C_{60}, a known Lewis acid,[48] in combination with NHC bases, for LPP of MMA and γ-MMBL; no polymerization was observed up to 24 h in different solvents (runs 17–18, Table 3).

Turning our attention to the scope of Lewis bases and considering the success of the $Al(C_6F_5)_3/P^tBu_3$ pair for LPP of various types of monomers, we were interested in the potential of chiral chelating phosphines for enhancements in activity and/or stereoselectivity in LPP. To this end, four chiral phosphines (Chart 1) were selected and investigated for MMA polymerization as LB components of LPs with $Al(C_6F_5)_3$. In comparison, CP-1, a chiral biNAP diphosphine, is much less active (TOF = 224 h^{-1}, run 1, Table 4) than P^tBu_3 (TOF = 1.2 × 10^4 h^{-1}). In addition, the polymer produced exhibited a bimodal MWD, with M_n = 3.70 × 10^5 g mol^{-1}, PDI = 1.13 (56%) and M_n = 1.29 × 10^6 g mol^{-1}, PDI = 1.01 (44%). CP-2, a benzene-bridged diphosphine, showed a 3.5-fold activity enhancement over CP-1 (run 2 *vs.* 1), but it is still less active than the simple P^tBu_3. Impressively, CP-3, an ethylene-bridged diphosphine, is 4 times more active than P^tBu_3, achieving a high TOF of 4.8 × 10^4 h^{-1} (run 3, Table 4). The PMMA produced also had a high MW of M_n = 2.74 × 10^5 g mol^{-1} and a unimodal MWD (PDI = 1.40). The analogous 2,3-butane-bridged chiral diphosphine, CP-4, is also highly active, achieving a high TOF of 1.6 × 10^4 h^{-1} and a high MW of M_n = 3.68 × 10^5 g mol^{-1} (PDI = 1.48, run 4, Table 4). In all cases, the syndiotacticity of PMMA produced by these chiral LB/LA pairs was about 74–75% rr, showing no enhancement over the PMMA produced by the achiral $Al(C_6F_5)_3/P^tBu_3$ pair.

Superbases, P_4-^{t}Bu and P_2-^{t}Bu (Chart 1), were also investigated as LBs for LPP of MMA. The $Al(C_6F_5)_3/P_4$-^{t}Bu pair exhibited the *highest* activity amongst all LPs investigated in this study, giving the highest TOF of 9.6 × 10^4 h^{-1} (*i.e.*, consuming all 800 equiv. of monomer in 30 s!) and also producing high MW PMMA with M_n = 2.12 × 10^5 g mol^{-1} and narrow MWD of PDI = 1.34 (run 5, Table 4). The $Al(C_6F_5)_3/P_2$-^{t}Bu pair is also highly active with TOF = 4.8 × 10^4 h^{-1} (run 6, Table 4). On the other hand, the LPs of $Al(C_6F_5)_3$ with two tertiary amines, NPh_3 and NEt^iPr_2, showed no activity toward polymerization of MMA up to 24 h (runs 7–8). The $Al(C_6F_5)_3/NPh_3$ pair is also inactive for the polymerization of the more reactive monomer γ-MMBL (run 9), but the $Al(C_6F_5)_3/NEt^iPr_2$ pair exhibits good activity for polymerization of γ-MMBL, achieving quantitative conversion in 5 h and giving a TOF of 160 h^{-1} (run 10, Table 4).

Computational studies of zwitterionic active species formation, chain initiation and propagation

This section focuses on the mechanistic aspects of $Al(C_6F_5)_3$-based LPs as catalysts in MMA polymerization. The LB/Al $(C_6F_5)_3$ pairs, LB = phosphines (P^tBu_3, $PMes_3$ and PPh_3) and NHC (IMes), were examined for their formation of the active species upon reaction with the monomer MMA as well as subsequent MMA addition to the formed zwitterionic active species.

Zwitterion formation and stability. We started from MMA coordination to the Al atom of $Al(C_6F_5)_3$ to form the alane-activated monomer adduct [Al]–MMA. Next, we considered the reaction of the adduct with different LBs to form the zwitterionic active species [Al]–MMA–LB. The energetics of these steps is shown in Scheme 2. Here we report the energy values obtained with both BP86 and M06 functionals. The former is known to underestimate binding energy but offers a balanced approach when the binding of different large ligands is compared. Conversely, the latter predicts much more reasonable binding energies, but has some tendency to overestimate the binding energy of large ligands in solution.[49]

Despite the unfavorable entropic contribution due to MMA coordination to $Al(C_6F_5)_3$, formation of the [Al]–MMA adduct, which was previously isolated and structurally characterized,[9,25] is strongly favored, with a binding energy of the alane to MMA of 25.7 and 38.2 kcal mol^{-1} at the BP86 and M06 levels,

Published on 22 May 2012. Downloaded by UNIVERSITY OF TEESSIDE on 09/10/2014 08:42:21.

Table 4 Polymerization results by $Al(C_6F_5)_3$/LB pairs[a]

Run no.	LB (1 eq.)	Monomer (M)	[M]/[LB]	Solvent	Time (min)	Conv.[b] (%)	TOF (h^{-1})	10^{-4} M_n[c] (g mol^{-1})	PDI[c] (M_w/M_n)	[rr][d] (%)
1	CP-1	MMA	800	Toluene	210	98.0	224	37.0 (56%)	1.13	74.7
2	CP-2	MMA	800	Toluene	60	98.3	786	25.8	1.83	73.8
3	CP-3	MMA	800	Toluene	1	100	48 000	27.4	1.40	73.7
4	CP-4	MMA	800	Toluene	3	100	16 000	36.8	1.48	74.2
5	P_4-^{t}Bu	MMA	800	Toluene	0.5	100	96 000	21.2	1.34	72.4
6	P_2-^{t}Bu	MMA	400	Toluene	0.5	100	48 000	4.82	1.64	72.8
7	NPh_3	MMA	800	CH_2Cl_2	1440	0	0	—	—	—
8	NEt^iPr_2	MMA	800	CH_2Cl_2	1440	0	0	—	—	—
9	NPh_3	γ-MMBL	800	CH_2Cl_2	1440	0	0	—	—	—
10	NEt^iPr_2	γ-MMBL	800	CH_2Cl_2	300	100	160	9.77	1.90	n/a

[a] Conditions: [LA]/[LB] = 2, LA = $Al(C_6F_5)_3$ as a toluene adduct; RT (~25 °C). n/a = not applicable. [b] Monomer conversions measured by ^{1}H NMR. [c] Number-average molecular weight (M_n) and polydispersity index (PDI) determined by GPC relative to PMMA standards; values (percentages) in parentheses were the percentage of the major peak when the other minor shoulder peak showed up on the GPC trace. [d] Polymer methyl triads (rr, mr, mm) measured by ^{1}H NMR.

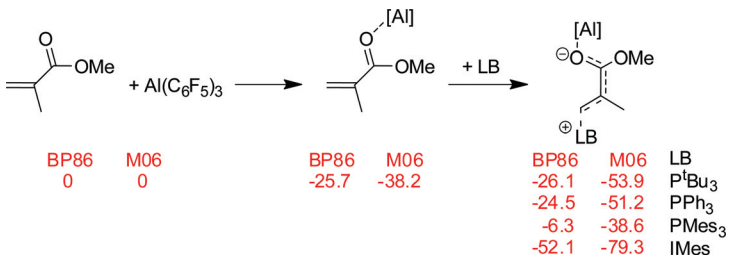

Scheme 2 Energetics (kcal mol^{-1}) of zwitterion formation with different LBs, as predicted by the BP86 and M06 functionals. Separated MMA, $Al(C_6F_5)_3$ and LB is assumed as the reference system at 0 kcal mol^{-1}.

respectively (Scheme 2). This result was expected considering the extremely high Lewis acidity of $Al(C_6F_5)_3$.[7,11,50] The energetics of the zwitterion formation largely depends on the LB and the functional considered. In fact, as shown in Scheme 2, binding of IMes to the [Al]–MMA adduct is strongly favored, with the zwitterionic species [Al]–MMA–IMes more than 50 kcal mol^{-1} below the starting species, with a net gain of roughly 26 kcal mol^{-1} from the [Al]–MMA adduct, while phosphines bind much less strongly to the [Al]–MMA adduct, with the binding strongly influenced by the functional. For instance, the BP86 functional predicts an energy gain of only 0.4 for P^tBu_3, whereas binding of PPh_3 and $PMes_3$ to the [Al]–MMA adduct is unfavored by 1.2 and 19.4 kcal mol^{-1}, respectively. Considering an unfavorable entropic contribution, not considered in the present case, the [Al]–MMA–PR_3 zwitterion is predicted to be unstable at the BP86 level. Differently, a sizeable zwitterion energy formation is predicted by the M06 functional, with the binding of all the LBs to the [Al]–MMA moiety being roughly 15 kcal mol^{-1} stronger. Consequently, even including an unfavorable entropic contribution, formation of [Al]–MMA–PR_3 (R = ^{t}Bu, Ph) zwitterions is favored with the M06 functional, while $PMes_3$ is unbound to the adduct, in agreement with experiments. It is worth noting that the relative stability of the phosphine zwitterion species predicted by both the BP86 and the M06 functionals is in good agreement with the experimental results, which showed somewhat greater stability of the P^tBu_3 zwitterion species relative to the PPh_3 zwitterion as well as no zwitterion formation in the case of $PMes_3$ and no polymerization activity by the $Mes_3P/Al(C_6F_5)_3$ pair. The instability of the

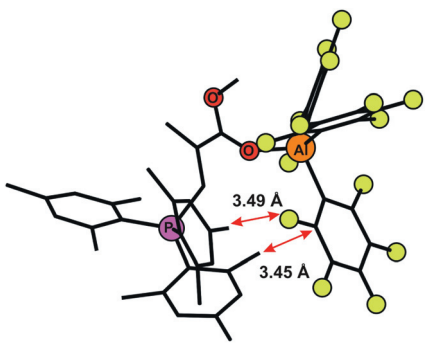

Fig. 6 DFT optimized geometry of the $Al(C_6F_5)_3$–MMA–$PMes_3$ zwitterion.

$PMes_3$ zwitterion can be easily explained considering the optimized geometry shown in Fig. 6, where repulsive steric interaction between the methyl substituents on the mesityl rings and the phenyl groups of $Al(C_6F_5)_3$, due to the short distances between these groups, are responsible for the zwitterion instability.

If similar stability of the [Al]–MMA–PPh_3 and [Al]–MMA–P^tBu_3 zwitterionic species was expected, there would be no meaningful steric interaction between the alane and the base that can justify the different stability of the zwitterions derived from IMes and PR_3. Indeed, the energy gain associated with addition of the small PMe_3 to the [Al]–MMA adduct is 7.4 and 14.6 kcal mol^{-1} at the BP86 and M06 levels, which indicates that steric repulsion somewhat destabilizes the binding of the larger P^tBu_3

 This journal is © The Royal Society of Chemistry 2012

Published on 22 May 2012. Downloaded by UNIVERSITY OF TEESSIDE on 09/10/2014 08:42:21.

Table 5 Natural bond orbital and bond strength analysis of [Al]–MMA–PPh_3 and [Al]–MMA–IMes zwitterionic species

	[Al]–MMA–PPh_3	[Al]–MMA–IMes
Bond length C_{MMA}–LB (Å)	1.94	1.50
Bond order C_{MMA}–LB	0.83	1.04
Bond length O_{MMA}–Al (Å)	1.83	1.83
Bond order O_{MMA}–Al	0.32	0.33
Charge on $Al(C_6F_5)_3$ (electrons)	−0.21	−0.21
Charge on MMA (electrons)	−0.70	−0.60
Charge on LB (electrons)	0.91	0.81

and PPh_3 phosphines with the BP86 functional, and that the main source of stabilization with the M06 functional is dispersive in nature (at the M06 level P^tBu_3 binds more strongly than PMe_3 to [Al]–MMA). Analysis of the bond strength and charge distribution on PPh_3 and IMes zwitterions clearly show that the higher stability of the NHC zwitterion mainly arises from electronic effects (see Table 5). As shown in Table 5, for both the PPh_3 and IMes zwitterions the distance between the coordinated C atom of MMA and the coordinating P or C atom of the PPh_3 and IMes is close to a classical P–C or C–C σ bond, 1.84 and 1.54 Å, respectively. However, the C_{NHC}–C_{MMA} bond order is 1.04 in case of IMes, whereas, in case of the P–C_{MMA} bond with PPh_3, the order is lower, around 0.83. This result indicates that the MMA–IMes interaction in the zwitterion has a very strong covalent character, while the MMA–PPh_3 interaction in the zwitterion is more dative in nature. The Al–MMA interaction in the zwitterion, instead, is quite similar for both PPh_3 and IMes. Natural Population Analysis (NPA) shows a slightly larger charge separation for the [Al]–MMA–PPh_3 with a greater positive charge on PPh_3, compared to the charge on IMes in the corresponding zwitterionic species. This analysis is consistent with a greater ionic character of the C_{MMA}–PPh_3 bond relative to the C_{MMA}–IMes bond.

The weaker stability of the PR_3-based zwitterions could be related to the experimentally observed bimodal molecular weight distribution of the PMMA obtained when the $Ph_3P/Al(C_6F_5)_3$ pair is employed as catalyst.[16] The formation of more than one active species could just arise from the decomposition of the [Al]–MMA–PPh_3 zwitterion.

MMA chain initiation. We move now to the addition of the first MMA molecule to the active [Al]–MMA–LB species for LB = PPh_3, P^tBu_3 and IMes, considering the two most probable mechanisms shown in Scheme 3. In the first pathway the zwitterion attacks an Al-free MMA molecule (monometallic mechanism, Scheme 3a), while in the second the zwitterion attacks an Al-activated MMA molecule, namely the preformed alane–monomer adduct (bimetallic mechanism, Scheme 3b). The energy barriers obtained with the BP86 and M06 functionals for the two mechanisms are also reported in Scheme 3.

The most stable transition states for MMA addition along the two reaction pathways shown in Scheme 3 are compared in Fig. 7 for the case of PPh_3-based zwitterionic species. Although the bimetallic TS displays a more crowded geometry, see the short distance between the LB and the $Al(C_6F_5)_3$ moiety coordinated to the monomer in Fig. 7b, the numbers in the Scheme 3 show clearly that whatever LB is considered, the bimetallic

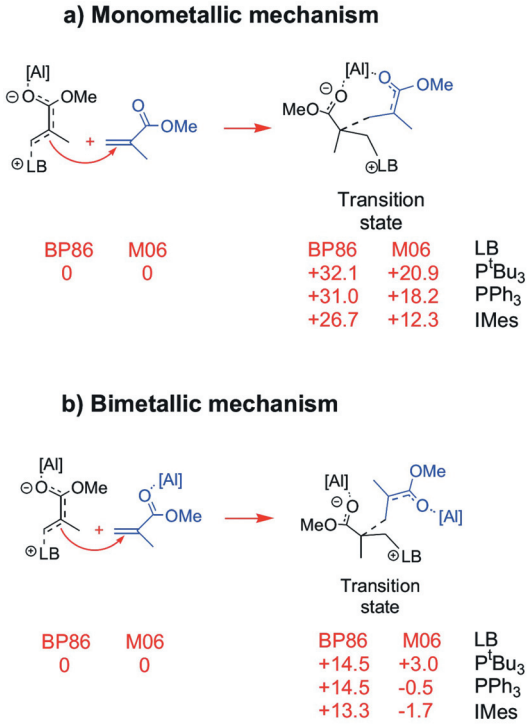

Scheme 3 Energetics (kcal mol^{-1}) of the first MMA addition to a preformed zwitterion with the BP86 and the M06 functionals.

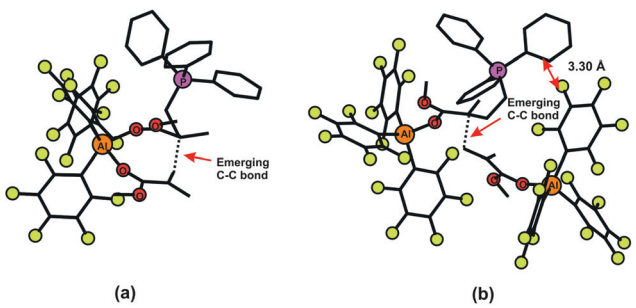

Fig. 7 Transition state geometries of MMA addition to the $Al(C_6F_5)_3$–MMA–PPh_3 zwitterion proceeding *via* the monometallic (a) and bimetallic (b) mechanisms.

mechanism is strongly favored, with an energy barrier roughly 15–20 kcal mol^{-1} lower than the energy barrier calculated for the monometallic mechanism. Both the BP86 and the M06 functionals performed consistently in this case.

The most notable difference between the M06 and BP86 results is that the BP86 functional, for both mechanisms, predicted energy barriers roughly 10–15 kcal mol^{-1} higher than the corresponding energy barriers predicted by the M06 functional. Furthermore, the M06 functional predicted a negligible or even negative (LB = PPh_3 and IMes) energy barrier in case of the bimetallic mechanism. This result is expected based on the previously discussed differences between the two functionals, with a tendency of the M06 functional to overestimate the dispersive interactions, which are generated at the level of the TS by the close proximity of the zwitterions and the monomer.[51] However,

Published on 22 May 2012. Downloaded by UNIVERSITY OF TEESSIDE on 09/10/2014 08:42:21.

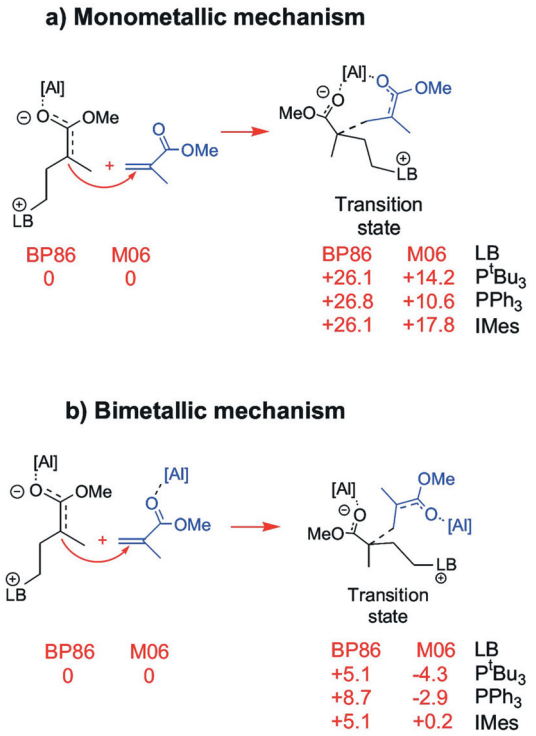

Scheme 4 Energetics (kcal mol^{-1}) of the generic MMA addition to a preformed zwitterion with the BP86 and the M06 functionals.

of paramount relevance here is the calculated preference for the bimetallic mechanism, whatever functional is considered, which is in agreement with the experimental data showing that the rate of MMA polymerization increases significantly by increasing the [Al]/LB ratio, and that the MMA reaction starts with a negligible induction period when the preformed zwitterion and [Al]–MMA adduct is employed (*vide supra*).

MMA chain propagation step. In this section we describe the reaction profile for MMA addition in a propagation step in the case of a long PMMA chain. The generic propagating active species was simulated by adding a methylene unit between the LB and the last inserted MMA molecule with a coordinated [Al] moiety, see Scheme 4. The addition of the methylene unit breaks connection between the LB and the [Al] through π-bonds, leaving only a σ-bond connection. The energy profiles for the mono- and the bimetallic MMA additions using PPh_3, P^{t}Bu$_3$ and IMes LBs are schematically shown in Scheme 4.

As anticipated, also in the chain growth step addition of the [Al]–MMA adduct is strongly favored, compared to the addition of non-activated MMA for all the LP systems considered. In fact, the numbers in Scheme 4 show a clear preference for the bimetallic mechanism with both functionals considered.[52] Comparison between the initiation step, Scheme 3, and the generic chain growth step, Scheme 4, indicates that in the generic chain growth step there is a reduction of roughly 10 kcal mol^{-1} in the energy barriers for both the mono and the bimetallic mechanisms, although this decrease is somewhat smaller in case of the M06 functional. The reduction of repulsive steric interaction between the Al(C$_6$F$_5$)$_3$ moiety coordinated to the monomer and the LB bonded to the growing chain, the latter being pushed away from the reacting atoms by the added methylene unit on the growing chain, mainly contributes to the reduced energy barrier for MMA addition.

Conclusions

Highly active and effective LPP systems have been achieved with classical and frustrated LPs based on the strong Lewis acid Al(C$_6$F$_5$)$_3$. Such CLPs and FLPs are especially effective for polymerizing conjugated polar alkenes such as MMA, acrylamides and especially renewable α-methylene-γ-butyrolactones MBL and γ-MMBL, into high MW polymers with relatively narrow MWDs. Investigations into the scope of LAs show that although some common LAs can also be utilized for LPP, Al(C$_6$F$_5$)$_3$-based LPs are far more active and effective than other LA-based LPs. On the other hand, the scope of LBs is not limited, and several types of LBs can also be utilized for establishing highly active and effective LPP systems employing Al(C$_6$F$_5$)$_3$. Such highly effective LBs include (listed here only MMA polymerization data for comparison): achiral phosphine P^{t}Bu$_3$ (TOF = 1.2 × 10^4 h^{-1} M_n = 3.97 × 10^5 g mol^{-1}, PDI = 1.52), chiral ethylene-bridged diphosphine CP-3 (TOF = 4.8 × 10^4 h^{-1}, M_n = 2.74 × 10^5 g mol^{-1}, PDI = 1.40), NHC bases IMes (TOF = 4.8 × 10^4 h^{-1}, M_n = 2.66 × 10^4 g mol^{-1}, PDI = 1.77), I^{t}Bu (TOF = 3.2 × 10^3 h^{-1}, M_n = 5.25 × 10^5 g mol^{-1}, PDI = 1.43), and TPT, as well as the superbase P$_4$-^{t}Bu, which is most active (TOF = 9.6 × 10^4 h^{-1}, M_n = 2.12 × 10^5 g mol^{-1}, PDI = 1.34). These LPs are also highly active and effective for polymerization of γ-MMBL, observing the similar effect of the NHC base structure on the resulting polymer MW (*e.g.*, the MW of the polymer by I^{t}Bu is much higher than that by IMes). In terms of stereoselectivity of these LPP systems, the polymers produced at RT are typically atactic (PMMBL with ~47% mr) or syndio-rich (PMMA with ~70–75% rr). The use of chiral chelating phosphine bases did not noticeably affect the stereoselectivity. However, highly syndiotactic PMMA with 91.% rr can be produced by chiral or achiral LPs at −78 °C.

Mechanistic studies have identified and structurally characterized zwitterionic phosphonium and imidazolium enolaluminate species, formed by the reaction of the monomer·Al(C$_6$F$_5$)$_3$ adduct with P^{t}Bu$_3$ and NHCs, respectively. Such zwitterions were proposed to be the active species for the polymerization because they rapidly polymerize the subsequently added monomer. Kinetic studies have revealed that the MMA polymerization by the most representative LP of the current systems, ^{t}Bu$_3$P/Al(C$_6$F$_5$)$_3$ is zero-order in monomer concentration after an initial induction period and the polymerization is significantly catalyzed by the LA, conforming to a bimolecular, activated monomer propagation mechanism.

Computational work has examined the energetics of the zwitterionic active species formation as well as chain initiation and propagation fundamental steps involved in LPP. Consistent with experimental results, formation of the zwitterion is favored with all the LBs considered, with the exception of PMes$_3$, due to the bulkiness of the mesityl groups. Analysis of the chain initiation step indicated that the bimetallic mechanism, with addition of a LA-activated MMA molecule to the zwitterion, is clearly favored over the monometallic mechanism involving addition of a non-activated MMA. Analysis of a model of the MMA

 This journal is © The Royal Society of Chemistry 2012

Published on 22 May 2012. Downloaded by UNIVERSITY OF TEESSIDE on 09/10/2014 08:42:21.

propagation step confirmed the preference for the bimetallic mechanism, with an overall reduction of the addition energy barrier, which is a consequence of the reduced steric stress induced by the more spatially separated LA and LB centers. The main difference between the NHC and the PR_3 based LPP systems is in the relative stability of the zwitterion, while the behavior in MMA addition is remarkably similar.

Acknowledgements

This work was supported by the National Science Foundation (CHE 1150792) for the study carried out at Colorado State University. MGJ thanks NSF-REU (CHE 1004924) for support of summer research. LC thanks the HPC team of Enea (www.enea.it) for using the ENEA-GRID and the HPC facilities CRESCO (www.cresco.enea.it) in Portici, Italy. We thank Boulder Scientific Co. for the research gifts of $B(C_6F_5)_3$ and $[Ph_3C][B(C_6F_5)_4]$, and Dr. Brian Newell for the help on the X-ray structural analysis.

References

1 For recent reviews, see: (*a*) D. W. Stephan and G. Erker, *Angew. Chem., Int. Ed.*, 2010, **49**, 46–76; (*b*) G. Erker, *Dalton Trans.*, 2011, **40**, 7475–7483.

2 (*a*) J. S. J. McCahill, G. C. Welch and D. W. Stephan, *Angew. Chem., Int. Ed.*, 2007, **46**, 4968–4971; (*b*) P. A. Chase, G. C. Welch, T. Jurca and D. W. Stephan, *Angew. Chem., Int. Ed.*, 2007, **46**, 8050–8053; (*c*) G. C. Welch and D. W. Stephan, *J. Am. Chem. Soc.*, 2007, **129**, 1880–1881; (*d*) P. Spies, G. Erker, G. Kehr, K. Bergander, R. Fröhlich, S. Grimme and D. W. Stephan, *Chem. Commun.*, 2007, 5072–5074; (*e*) G. C. Welch, R. R. S. Juan, J. D. Masuda and D. W. Stephan, *Science*, 2006, **314**, 1124–1126.

3 For selected recent examples on activation of small molecules by FLPs, see: (*a*) F. Bertini, V. Lyaskovskyy, B. J. J. Timmer, F. J. J. de Kanter, M. Lutz, A. W. Ehlers, J. C. Slootweg and K. Lammertsma, *J. Am. Chem. Soc.*, 2012, **134**, 201–204; (*b*) A. Schäfer, M. Reiβmann, A. Schäfer, W. Saak, D. Haase and T. Müller, *Angew. Chem., Int. Ed.*, 2011, **50**, 12636–12638; (*c*) Z. Lu, Z. Cheng, Z. Chen, L. Weng, Z. H. Li and H. Wang, *Angew. Chem., Int. Ed.*, 2011, **50**, 12227–122231; (*d*) S. Kronig, E. Theuergarten, D. Holschumacher, T. Bannenberg, C. G. Daniliuc, P. G. Jones and M. Tamm, *Inorg. Chem.*, 2011, **50**, 7344–7359; (*e*) W. E. Piers, A. J. V. Marwitz and L. G. Mercier, *Inorg. Chem.*, 2011, **50**, 12252–12262; (*f*) X. Zhao and D. W. Stephan, *Chem. Commun.*, 2011, **47**, 1833–1835; (*g*) O. Ekkert, G. Kehr, R. Fröhlich and G. Erker, *J. Am. Chem. Soc.*, 2011, **133**, 4610–4616; (*h*) A. J. V. Marwitz, J. L. Dutton, L. G. Mercier and W. E. Piers, *J. Am. Chem. Soc.*, 2011, **133**, 10026–10029; (*i*) R. C. Neu, E. Otten, A. Lough and D. W. Stephan, *Chem. Sci.*, 2011, **2**, 170–176; (*j*) C. Appelt, H. Westenberg, F. Bertini, A. W. Ehlers, J. C. Slootweg, K. Lammertsma and W. Uhl, *Angew. Chem., Int. Ed.*, 2011, **50**, 3925–3928; (*k*) S. Grimme, H. Kruse, L. Goerigk and G. Erker, *Angew. Chem., Int. Ed.*, 2010, **49**, 1402–1405; (*l*) B. Inés, S. Holle, R. Goddard and M. Alcarazo, *Angew. Chem., Int. Ed.*, 2010, **49**, 8389–8391; (*m*) C. M. Mömming, E. Otten, G. Kehr, R. Fröhlich, S. Grimme, D. W. Stephan and G. Erker, *Angew. Chem., Int. Ed.*, 2009, **48**, 6643–6646; (*n*) M. A. Dureen, G. C. Welch, T. M. Gilbert and D. W. Stephan, *Inorg. Chem.*, 2009, **48**, 9910–9917; (*o*) M. A. Dureen, T. M. Gilbert and D. W. Stephan, *Chem. Commun.*, 2008, 4303–4305; (*p*) P. A. Chase and D. W. Stephan, *Angew. Chem., Int. Ed.*, 2008, **47**, 7433–7437; (*q*) D. Holschumacher, T. Bannenberg, C. G. Hrib, P. G. Jones and M. Tamm, *Angew. Chem., Int. Ed.*, 2008, **47**, 7428–7432; (*r*) V. Sumerin, F. Schulz, M. Nieger, M. Leskela, T. Repo and B. Rieger, *Angew. Chem., Int. Ed.*, 2008, **47**, 6001–6003.

4 For selected recent examples on catalytic hydrogenation by FLPs, see: (*a*) G. Erős, K. Nagy, H. Mehdi, I. Pápai, P. Nagy, P. Király, G. Tárkányi and T. Soós, *Chem.–Eur. J.*, 2012, **18**, 574–585; (*b*) D. W. Stephan, S. Greenberg, T. W. Graham, P. Chase, J. J. Hastie, S. J. Geier, J. M. Farrell, C. C. Brown, Z. M. Heiden, G. C. Welch and M. Ullrich, *Inorg. Chem.*, 2011, **50**, 12338–12348; (*c*) D. Chen, Y. Wang and J. Klankermayer, *Angew. Chem., Int. Ed.*, 2010, **49**, 9475–9478; (*d*) Z. M. Heiden and D. W. Stephan, *Chem. Commun.*, 2011, **47**, 5729–5731; (*e*) D. Chen, Y. Wang and J. Klankermayer, *Angew. Chem., Int. Ed.*, 2010, **49**, 9475–9478; (*f*) G. Erős, H. Mehdi, I. Pápai, T. A. Rokob, P. Király, G. Tárkányi and T. Soós, *Angew. Chem., Int. Ed.*, 2010, **49**, 6559–6563; (*g*) A. J. M. Miller, J. A. Labinger and J. E. Bercaw, *J. Am. Chem. Soc.*, 2010, **132**, 3301–3303; (*h*) A. W. Ashley, A. L. Thompson and D. O'Hare, *Angew. Chem., Int. Ed.*, 2009, **48**, 9839–9843; (*i*) K. V. Axenov, G. Kehr, R. Fröhlich and G. Erker, *J. Am. Chem. Soc.*, 2009, **131**, 3454–3455.

5 For selected recent examples on new reactivity/reaction development with FLPs, see: (*a*) B.-H. Xu, C. M. Mömming, R. Fröhlich, G. Kehr and G. Erker, *Chem.–Eur. J.*, 2012, **18**, 1826–1830; (*b*) A. J. P. Cardenas, B. J. Culotta, T. H. Warren, S. Grimme, A. Stute, R. Fröhlich, G. Kehr and G. Erker, *Angew. Chem., Int. Ed.*, 2011, **50**, 7567–7571; (*c*) A. M. Chapman, M. F. Haddow and D. F. Wass, *J. Am. Chem. Soc.*, 2011, **133**, 8826–8829; (*d*) G. Ménard and D. W. Stephan, *Angew. Chem., Int. Ed.*, 2011, **50**, 8396–8399; (*e*) X. Zhao and D. W. Stephan, *J. Am. Chem. Soc.*, 2011, **133**, 12448–12450; (*f*) C. M. Mömming, G. Kehr, R. Fröhlich and G. Erker, *Chem. Commun.*, 2011, **47**, 2006–2007; (*g*) G. Ménard and D. W. Stephan, *J. Am. Chem. Soc.*, 2010, **132**, 1796–1797; (*h*) M. Alcarazo, C. Gomez, S. Holle and R. Goddard, *Angew. Chem., Int. Ed.*, 2010, **49**, 5788–5791; (*i*) A. Berkefeld, W. E. Piers and M. Parvez, *J. Am. Chem. Soc.*, 2010, **132**, 10660–10661; (*j*) C. M. Mömming, G. Kehr, B. Wibbeling, R. Fröhlich, B. Schirmer, S. Grimme and G. Erker, *Angew. Chem., Int. Ed.*, 2010, **49**, 2414–2417.

6 E. Y.-X. Chen, in *e-EROS Encyclopedia of Reagents for Organic Synthesis*, John Wiley & Sons, Ltd, West Sussex, UK, 2011, DOI: 10.1002/047084289X.rn01382.

7 E. Y.-X. Chen, W. J. Kruper, G. Roof and D. R. Wilson, *J. Am. Chem. Soc.*, 2001, **123**, 745–746.

8 E. Y.-X. Chen and K. A. Abboud, *Organometallics*, 2000, **19**, 5541–5543.

9 A. D. Bolig and E. Y.-X. Chen, *J. Am. Chem. Soc.*, 2001, **123**, 7943–7944.

10 D. Chakraborty and E. Y.-X. Chen, *Macromolecules*, 2002, **35**, 13–15.

11 G. S. Hair, A. H. Cowley, R. A. Jones, B. G. McBurnett and A. Voigt, *J. Am. Chem. Soc.*, 1999, **121**, 4922–4923.

12 (*a*) E. Y.-X. Chen, *Chem. Rev.*, 2009, **109**, 5157–5214; (*b*) E. Y.-X. Chen, *Dalton Trans.*, 2009, 8784–8793.

13 (*a*) Y. Zhang, L. O. Gustafson and E. Y.-X. Chen, *J. Am. Chem. Soc.*, 2011, **133**, 13674–13684; (*b*) Y. Hu, X. Xu, Y. Zhang, Y. Chen and E. Y.-X. Chen, *Macromolecules*, 2010, **43**, 9328–9336; (*c*) G. M. Miyake, S. E. Newton, W. R. Mariott and E. Y.-X. Chen, *Dalton Trans.*, 2010, **39**, 6710–6718; (*d*) R. A. Cockburn, T. F. L. McKenna and R. A. Hutchinson, *Macromol. Chem. Phys.*, 2010, **211**, 501–509; (*e*) J. Mosnáček and K. Matyjaszewski, *Macromolecules*, 2008, **41**, 5509–5511.

14 H. M. R. Hoffman and J. Rabe, *Angew. Chem., Int. Ed. Engl.*, 1985, **24**, 94–110.

15 (*a*) L. E. Manzer, *ACS Symp. Ser.*, 2006, **921**, 40–51; (*b*) L. E. Manzer, *Appl. Catal. A: Gen.*, 2004, **272**, 249–256.

16 Y. Zhang, G. M. Miyake and E. Y.-X. Chen, *Angew. Chem., Int. Ed.*, 2010, **49**, 10158–10162.

17 Y. Zhang, G. M. Miyake and E. Y.-X. Chen, *Angew. Chem., Int. Ed.*, 2012, **51**, 2465–2469.

18 Group transfer polymerization of MMA initiated by silyl ketene acetals and catalyzed by nucleophilic NHCs, I^iPr and I^tBu, was recently reported in: (*a*) J. Raynaud, Y. Gnanou and D. Taton, *Macromolecules*, 2009, **42**, 5996–6005; (*b*) J. Raynaud, A. Ciolino, A. Baceiredo, M. Destarac, F. Bonnette, T. Kato, Y. Gnanou and D. Taton, *Angew. Chem., Int. Ed.*, 2008, **47**, 5390–5393; (*c*) M. D. Scholten, J. L. Hedrick and R. M. Waymouth, *Macromolecules*, 2008, **41**, 7399–7404.

19 Y. C. Kim, M. Jeon and S. Y. Kim, *Macromol. Rapid Commun.*, 2005, **26**, 1499–1503.

20 (*a*) D. Enders, K. Breuer, G. Raabe, J. Runsink, J. H. Teles, J. P. Melder, K. Ebel and S. Brode, *Angew. Chem., Int. Ed. Engl.*, 1995, **34**, 1021–1023; (*b*) D. Enders, K. Breuer, U. Kallfass and T. Balensiefer, *Synthesis*, 2003, 1292–1295.

21 A. P. Shreve, R. Mülhaupt, W. Fultz, J. Calabrese, W. Robbins and S. Ittel, *Organometallics*, 1988, **7**, 409–416.

22 D. Chakraborty and E. Y.-X. Chen, *Inorg. Chem. Commun.*, 2002, **5**, 698–701.

Published on 22 May 2012. Downloaded by UNIVERSITY OF TEESSIDE on 09/10/2014 08:42:21.

23 (*a*) M. Bochmann and S. J. Lancaster, *J. Organomet. Chem.*, 1992, **434**, C1–C5; (*b*) J. C. W. Chen, W.-M. Tsai and M. D. Rausch, *J. Am. Chem. Soc.*, 1991, **113**, 8570–8571.

24 (*a*) S. Feng, G. R. Roof and E. Y.-X. Chen, *Organometallics*, 2002, **21**, 832–839; (*b*) C. H. Lee, S. J. Lee, J. W. Park, K. H. Kim, B. Y. Lee and J. S. Oh, *J. Mol. Catal. A: Chem.*, 1998, **132**, 231–239; (*c*) P. Biagini, G. Lugli, L. Abis and P. Andreussi, *U.S. Pat.*, 5,602269, 1997.

25 A. Rodriguez-Delgado and E. Y.-X. Chen, *J. Am. Chem. Soc.*, 2005, **127**, 961–974.

26 *SHELXTL, Version 6.12*, Bruker Analytical X-ray Solutions, Madison, WI, 2001.

27 (*a*) A. Rodriguez-Delgado and E. Y.-X. Chen, *Macromolecules*, 2005, **38**, 2587–2594; (*b*) A. D. Bolig and E. Y.-X. Chen, *J. Am. Chem. Soc.*, 2004, **126**, 4897–4906.

28 (*a*) A. Rodriguez-Delgado, W. R. Mariott and E. Y.-X. Chen, *Macromolecules*, 2004, **37**, 3092–3100; (*b*) F. A. Bovey and P. A. Mirau, *NMR of Polymers*, Academic Press, San Diego, CA, 1996; (*c*) R. Subramanian, R. D. Allen, J. E. McGrath and T. C. Ward, *Polym. Prepr. (Am. Chem. Soc., Div. Polym. Chem.)*, 1985, **26**, 238–240.

29 (*a*) G. M. Miyake, Y. Zhang and E. Y.-X. Chen, *Macromolecules*, 2010, **43**, 4902–4908; (*b*) J. Suenaga, D. M. Sutherlin and J. K. Stille, *Macromolecules*, 1984, **17**, 2913–2916.

30 M. J. Frisch, G. W. Trucks, H. B. Schlegel, G. E. Scuseria, M. A. Robb, J. R. Cheeseman, G. Scalmani, V. Barone, B. Mennucci, G. A. Petersson, H. Nakatsuji, M. Caricato, X. Li, H. P. Hratchian, A. F. Izmaylov, J. Bloino, G. Zheng, J. L. Sonnenberg, M. Hada, M. Ehara, K. Toyota, R. Fukuda, J. Hasegawa, M. Ishida, T. Nakajima, Y. Honda, O. Kitao, H. Nakai, T. Vreven, J. A. Montgomery, Jr., J. E. Peralta, F. Ogliaro, M. Bearpark, J. J. Heyd, E. Brothers, K. N. Kudin, V. N. Staroverov, R. Kobayashi, J. Normand, K. Raghavachari, A. Rendell, J. C. Burant, S. S. Iyengar, J. Tomasi, M. Cossi, N. Rega, J. M. Millam, M. Klene, J. E. Knox, J. B. Cross, V. Bakken, C. Adamo, J. Jaramillo, R. Gomperts, R. E. Stratmann, O. Yazyev, A. J. Austin, R. Cammi, C. Pomelli, J. Ochterski, R. L. Martin, K. Morokuma, V. G. Zakrzewski, G. A. Voth, P. Salvador, J. J. Dannenberg, S. Dapprich, A. D. Daniels, O. Farkas, J. B. Foresman, J. V. Ortiz, J. Cioslowski and D. J. Fox, *GAUSSIAN 09*, Gaussian, Inc., Wallingford, CT, 2009.

31 (*a*) A. D. Becke, *Phys. Rev. A*, 1988, **38**, 3098–3100; (*b*) J. P. Perdew, *Phys. Rev. B*, 1986, **33**, 8822–8824; (*c*) J. P. Perdew, *Phys. Rev. B*, 1986, **34**, 7406–7406.

32 F. Weigend and R. Ahlrichs, *Phys. Chem. Chem. Phys.*, 2005, **7**, 3297–3305.

33 (*a*) Y. Zhao and D. G. Truhlar, *Theor. Chem. Acc.*, 2008, **120**, 215–241; (*b*) Y. Zhao and D. G. Truhlar, *J. Chem. Phys.*, 2006, **125**, 194101–194118.

34 (*a*) J. Tomasi, B. Mennucci and R. Cammi, *Chem. Rev.*, 2005, **105**, 2999–3094; (*b*) V. Barone and M. Cossi, *J. Phys. Chem. A*, 1998, **102**, 1995–2001.

35 M. Ullrich, K. S.-H. Seto, A. J. Lough and D. W. Stephan, *Chem. Commun.*, 2009, 2335–2337.

36 M. A. Dureen and D. W. Stephan, *J. Am. Chem. Soc.*, 2009, **131**, 8396–8397.

37 B.-H. Xu, G. Kehr, R. Fröhlich, B. Wibbeling, B. Schirmer, S. Grimme and G. Erker, *Angew. Chem., Int. Ed.*, 2011, **50**, 7183–7186.

38 Y. Ning, H. Zhu and E. Y.-X. Chen, *J. Organomet. Chem.*, 2007, **692**, 4535–4544.

39 P. A. Chase and D. W. Stephan, *Angew. Chem., Int. Ed.*, 2008, **47**, 7433–7437.

40 D. Holschumacher, T. Bannenberg, C. G. Hrib, P. G. Jones and M. Tamm, *Angew. Chem., Int. Ed.*, 2008, **47**, 7428–7432.

41 (*a*) A. T. Biju, M. Padmanaban, N. E. Wurz and F. Glorius, *Angew. Chem., Int. Ed.*, 2011, **50**, 8412–8415; (*b*) S.-I. Matsuoka, Y. Ota, A. Washio, A. Katada, K. Ichioka, K. Takagi and M. Suzuki, *Org. Lett.*, 2011, **13**, 3722–3725.

42 Direct contact of DCM with $Al(C_6F_5)_3$ must be avoided as it results in decomposition leading to formation of $[ClAl(C_6F_5)_2]_2$: D. Chakraborty and E. Y.-X. Chen, *Inorg. Chem. Commun.*, 2002, **5**, 698–701. On the other hand, The $Al(C_6F_5)_3$-monomer adducts (either isolated or *in situ* generated) are inert towards DCM.

43 (*a*) Y. Ning, M. J. Cooney and E. Y.-X. Chen, *J. Organomet. Chem.*, 2005, **690**, 6263–6270; (*b*) G. Stojcevic, H. Kim, N. J. Taylor, T. B. Marder and S. Collins, *Angew. Chem., Int. Ed.*, 2004, **43**, 5523–5526; (*c*) Y. Li, D. G. Ward, S. S. Reddy and S. Collins, *Macromolecules*, 1997, **30**, 1875–1883.

44 E. Y.-X. Chen, *Dalton Trans.*, 2009, 8784–8793.

45 (*a*) Y. Zhang and E. Y.-X. Chen, *Macromolecules*, 2008, **41**, 36–42; (*b*) Y. Zhang and E. Y.-X. Chen, *Macromolecules*, 2008, **41**, 6353–6360.

46 Some activity (TOF < 2 h^{-1}) was observed for MMA polymerization by R_3P–Et_3Al at low temperatures (−78 °C or −93 °C): T. Kitayama, E. Masuda, M. Yamaguchi, T. Nishiura and K. Hatada, *Polym. J.*, 1992, **24**, 817–827.

47 E. Y.-X. Chen and T. J. Mark, *Chem. Rev.*, 2000, **100**, 1391–1434.

48 (*a*) J. Iglesias-Sigüenza and M. Alcarazo, *Angew. Chem., Int. Ed.*, 2012, **51**, 2–4; (*b*) H. Li, C. Risko, J. H. Seo, C. Campbell, G. Wu, J.-L. Brédas and G. C. Bazan, *J. Am. Chem. Soc.*, 2011, **133**, 12410–12413.

49 (*a*) H. Jacobsen and L. Cavallo, *ChemPhysChem*, 2012, **13**, 562–569; (*b*) S. Torker, D. Merki and P. Chen, *J. Am. Chem. Soc.*, 2008, **130**, 4808–4814; (*c*) D. Benitez, E. Tkatchouk and W. W. Goddard, *Chem. Commun.*, 2008, 6194–6196; (*d*) Y. Zhao and D. G. Truhlar, *Org. Lett.*, 2007, **9**, 1967–1970.

50 (*a*) A. Y. Timoshkin and G. Frenking, *Organometallics*, 2008, **27**, 371–380; (*b*) K. Vanka, M. S. W. Chan, C. C. Pye and T. Ziegler, *Organometallics*, 2000, **19**, 1841–1849.

51 We have also tested the M05-2X functional in the calculation of the first transition state energy barrier. This functional is largely used in describing the reactivity with the FLP systems: (*a*) F. Huang, G. Lu, L. Zhao, H. Li and Z.-X. Wang, *J. Am. Chem. Soc.*, 2010, **132**, 12388–12396; (*b*) T. A. Rokob, A. Hamza and I. Pàpai, *J. Am. Chem. Soc.*, 2009, **131**, 10702–10710. The energy barrier for the bimetallic mechanism for the IMes-based system increases to 0.2 kcal mol^{-1} with the M05-2X functional with respect to −1.7 kcal mol^{-1} with the M06 functional.

52 For all systems the energy barriers calculated at BP86 level for the bimetallic mechanism are comparable to the energy barrier we calculated for MMA addition with metallocene catalysts, see: (*a*) Y. Ning, L. Caporaso, A. Correa, L. O. Gustafson, L. Cavallo and E. Y.-X. Chen, *Macromolecules*, 2008, **41**, 6910–6919; (*b*) L. Caporaso and L. Cavallo, *Macromolecules*, 2008, **41**, 3439–3445; (*c*) L. Caporaso, J. Gracia-Budrìa and L. Cavallo, *J. Am. Chem. Soc.*, 2006, **128**, 16649–16654.

 This journal is © The Royal Society of Chemistry 2012